

Sensory-specific modulation of adult neurogenesis in sensory structures is associated with the type of stem cell present in the neurogenic niche of the zebrafish brain

Benjamin W. Lindsey,¹ Sabrina Di Donato,² Jan Kaslin¹ and Vincent Tropepe²

¹Australian Regenerative Medicine Institute, Monash University Clayton Campus, Clayton, Vic., Australia

²Department of Cell and Systems Biology, University of Toronto, 25 Harbord Street, Toronto, ON M5S 3G5, Canada

Keywords: adult neural stem cells, adult neurogenesis, *Danio rerio*, neurogenic plasticity, sensory enrichment/deprivation

Abstract

Teleost fishes retain populations of adult stem/progenitor cells within multiple primary sensory processing structures of the mature brain. Though it has commonly been thought that their ability to give rise to adult-born neurons is mainly associated with continuous growth throughout life, whether a relationship exists between the processing function of these structures and the addition of new neurons remains unexplored. We investigated the ultrastructural organisation and modality-specific neurogenic plasticity of niches located in chemosensory (olfactory bulb, vagal lobe) and visual processing (periventricular grey zone, torus longitudinalis) structures of the adult zebrafish (*Danio rerio*) brain. Transmission electron microscopy showed that the cytoarchitecture of sensory niches includes many of the same cellular morphologies described in forebrain niches. We demonstrate that cells with a radial-glia phenotype are present in chemosensory niches, while the niche of the caudal tectum contains putative neuroepithelial-like cells instead. This was supported by immunohistochemical evidence showing an absence of glial markers, including glial fibrillary acidic protein, glutamine synthetase, and S100 β in the tectum. By exposing animals to sensory assays we further illustrate that stem/progenitor cells and their neuronal progeny within sensory structures respond to modality-specific stimulation at distinct stages in the process of adult neurogenesis – chemosensory niches at the level of neuronal survival and visual niches in the size of the stem/progenitor population. Our data suggest that the adult brain has the capacity for sensory-specific modulation of adult neurogenesis and that this property may be associated with the type of stem cell present in the niche.

Introduction

Vertebrate adult neurogenesis can be modulated through changes in proliferation, survival or differentiation, and this appears to be associated with distinct functional requirements for new neurons (Grandel & Brand, 2013). Outside of mammals and birds however, there is little understanding of how adult neurogenesis may function as a biological substrate to modify species behaviour or information processing.

Studies of neurogenesis in the adult zebrafish forebrain have demonstrated that the cell types within neurogenic niches consist of populations of proliferative and non-proliferative glia that can be classified using immunohistochemical markers, with the stem/progenitor phenotype commonly having a radial glial (RG) profile (Ganz *et al.*, 2010; Marz *et al.*, 2010). Transmission electron microscopy (TEM) studies have revealed that the composition of different adult niches is further determined by the presence and frequency of seven distinct cell types (Type IIa–Type VI), with pallial niches characterised by Type IIa RG-like cells at the ventricular sur-

face and subpallial niches composed of layers of elongated Type III cells reminiscent of neuroepithelial (NE)-like profiles (Lindsey *et al.*, 2012). Accordingly, it has been documented that the cerebellum and optic tectum (TeO) also retain stem/progenitors with NE features similar to early development (Kaslin *et al.*, 2009, 2013; Alunni *et al.*, 2010; Ito *et al.*, 2010), though ultrastructural evidence for this is lacking.

As in the forebrain, constitutively active adult neurogenesis is also maintained in sensory structures of the teleost olfactory bulbs (OBs), vagal and facial lobes, and TeO (Zupanc *et al.*, 2005; Adolf *et al.*, 2006; Grandel *et al.*, 2006; Lindsey & Tropepe, 2006). Nevertheless, the ultrastructural composition and regulation of these niches, their properties of neurogenic plasticity, and whether a relationship exists between the processing capability of sensory structures and the phenotype of adult neural stem cells (ANSCs) remain unknown. Studies in cichlids have demonstrated that changes in cell proliferation rates in sensory and non-sensory niches appear to be coupled with social status (Maruska *et al.*, 2012). Recently, experiments investigating a link between the social environment and adult neurogenesis in telencephalic and sensory niches of the zebrafish have revealed that sensory niches are most influenced under contexts of social isolation or novelty, possibly because of differences in the

Correspondence: Vincent Tropepe, as above.
E-mail: v.tropepe@utoronto.ca

Received 7 May 2014, revised 8 August 2014, accepted 20 August 2014

degree of sensory stimuli (Lindsey & Tropepe, 2014). However, from this study it remained unresolved whether sensory niches were modulated by multimodal or unimodal stimuli.

Here, we used TEM and immunohistochemistry to investigate whether the cellular composition of niches in the OB, TeO and vagal lobe (LX) are conserved with cell types previously described in forebrain niches (Lindsey *et al.*, 2012). Furthermore, by exposing animals to specific chemosensory or visual stimuli we examined whether changes in ambient levels of modality-specific stimuli induced a widespread or niche-specific neurogenic response, and whether distinct stages of adult neurogenesis were affected. These experiments were aimed at testing the hypothesis that the adult zebrafish brain has the capability for sensory-specific neurogenic plasticity and that this may be associated with the cellular composition of the neurogenic niche.

Materials and methods

Animals

Wildtype zebrafish of both sexes (AB background; *n* total = 106: males, 76; females, 30) were used for all experiments unless stated otherwise, and maintained on a 14-h light : 10-h dark photoperiod at 28 °C in our fish facility (Aquaneering Inc., San Diego, CA, USA). Fish were fed a diet of granular food (ZM, Winchester, UK) and brine shrimp thrice daily. All zebrafish used for experiments were between 8 months and 1 year of age. Animals were killed using an overdose of 0.4% tricaine methanesulfonate diluted in tank water. Thereafter, the total body length (mm), weight (g) and sex of the fish were recorded. Handling procedures were done in accordance with the policies set forth by the University of Toronto and the Canadian Council for Animal Care (CCAC).

Chemosensory stimulant screening

To determine chemosensory stimulants (smell/taste) to which adult zebrafish responded we designed an assay to screen a variety of L-type amino acid combinations, bile salts and food extracts, previously suggested to elicit a response in zebrafish and other teleost species (Hara, 1994; Cachat *et al.*, 2010). All stimulants were obtained from Sigma, with the exception of dried bloodworms which were obtained locally at PetSmart (Toronto, ON, Canada). Mixtures of similar amino acids consisting of the same side chain were tested, including neutral amino acids (Cys, Gln, Met, Ser; 100 µM), basic amino acids (Arg, Lys, His; 300 µM), acidic amino acids (Asp, Glu; 100 µM) and hydrophobic aromatic amino acids (Phe, Trp, Tyr; 100 µM). Bile salts tested included sodium taurocholate hydrate (TCA) and its derivative, sodium taurodeoxycholate hydrate, both at final concentrations of 100 µM. Food extracts consisted of dried bloodworms, made by dissolving 50 g of crushed extract in 1 L of tank water and filtered to yield a final 0.02% solution. All concentrations given are for stimulants dissolved in 2 L tank water.

One day prior to chemosensory screening, fish were acclimated in individual 3-L testing tanks with a water volume of 2 L, and fasted for 24 h. Photoperiod and water temperature were maintained as above throughout the acclimation and testing period. The morning of testing, 10-mL aliquots of concentrated stimulants or vehicle control (tank water) were prepared fresh and warmed to 28 °C with testing commencing at 10:00 h. During stimulant screening single adult zebrafish were tested sequentially using 4.5-min-long trials and recorded from above using a JVC camcorder for downstream

analysis of the behavioural response (see Fig. 5A). The first 2 min of each trial was recorded to obtain a baseline of zebrafish swimming activity. Thereafter, 10 mL of chemosensory stimulant or vehicle was infused over a period of 20–30 s, and the response of zebrafish recorded for an additional 2 min. For each stimulant, a total of 6–10 fish were tested and 12 control trials were run.

Swimming behaviour was assessed using ETHOVISION 3.1, with the total distance travelled by zebrafish within the tank used to evaluate a response to chemosensory exposure. This method of assessment is one of a number of commonly used quantification methods to analyse swimming patterns in zebrafish under laboratory conditions (Blaser & Gerlai, 2006). We assumed that zebrafish would increase their swimming activity if a stimulant was detected, regardless of whether it was aversive or favorable, and as a result would increase the total path length travelled during the post-infusion trial period. To determine whether a significant difference was present before and after infusion of each stimulant, the total distance travelled (cm) was calculated by analysing the last minute pre-infusion and the first minute post-infusion and compared using a paired-samples *t*-test. Those stimulants producing a significant increase in swimming activity in zebrafish were then used to construct a chemosensory assay to test adult neurogenic plasticity.

Chemosensory assay used to test changes in adult neurogenesis

To investigate the effect of chemosensory stimulants on physiological levels of stem/progenitor cell proliferation, neuronal differentiation and neuronal survival in neurogenic niches residing in chemosensory processing structures, we exposed adult zebrafish to a randomised design of five different stimulants or tank water (vehicle control) over a 7-day period (see Fig. 6A). One day prior to exposure, animals were acclimated in testing tanks filled with tank water under standard housing conditions. Thereafter, over the 7-day exposure period zebrafish were randomly exposed to five different chemosensory stimulants (100 µM TCA, 100 µM acidic amino acids, 100 µM neutral amino acids, 100 µM aromatic amino acids or 0.02% bloodworms). All stimulants were warmed prior to infusion to 28 °C, the same temperature at which tanks were maintained. The first stimulant was administered at a volume of 10 mL at 08:00 h, with a different stimulant added thereafter every 2 h until 20:00 h. To avoid compounding of chemosensory stimulants, tanks were washed out daily with facility water for 30 min at 10:30, 13:30 and 20:30. This prevented poor water quality over the exposure period and, as well, allowed two or three stimulants to interact over a 4- to 6-h period and reduced the chances that fish habituated to similar combinations of stimulants.

Vision assay used to test changes in adult neurogenesis

To test the effect of a limited visual spectrum on physiological levels of stem/progenitor cell proliferation, neuronal differentiation and neuronal survival in neurogenic niches residing in visual processing structures, we exposed adult zebrafish to monochromatic light in the green (560 nm) or blue (480 nm) spectrum, in line with peak wavelengths reported for zebrafish cones (Fig. 7A; Fleisch & Neuhauss, 2006). Each monochromatic light condition was counterbalanced with full spectrum light normalised to the same light intensity using a Fisher Brand Light Meter (Fisher Scientific, Ottawa, ON, Canada): green light, ~200 lux; blue light, ~15 lux. For these studies, the same fiber optic light source and bulbs (21 volt; 150 watt; Ushio Halogen projector lamp) were used for experimen-

tal and control conditions, with the assumption that bulbs provided animals with near full spectrum light. Monochromatic light within chambers was achieved by shining fiber optic lights through band-pass filters (Asahi Spectra Co., Ltd., Tokyo, Japan) positioned on the lids of testing chambers. One day prior to exposure, zebrafish were placed in 2.5 L of tank water in standard housing tanks, and tanks placed into grey light-tight testing chambers. For the purposes of acclimation, lids were removed from chambers for 24 h prior to exposure. Each housing tank was equipped with PVC tubing for inflow and outflow to allow for water changes, and digital thermometers to monitor that water temperature remained at 28 °C. Room lights and fiber optic lights were set to a 14 h light (08:00–10:00 h) : 10 h dark (10:00–08:00 h) photoperiod. During the 7-day exposure period, zebrafish were housed in light-tight chambers under experimental (monochromatic) or control (full spectrum) conditions, with lids opened twice at 08:00 and 17:00 h for feeding, and a 1-L water change performed daily at 12:00 h.

Experimental design used to test different stages of adult neurogenesis

Chemosensory and vision assays were applied similarly according to the stage of adult neurogenesis investigated. To examine changes in stem/progenitor cell proliferation and neuronal differentiation, animals were exposed to assays over days 1–7. At 10:00 h on day 8, specimens were injected with a 10-mm bolus of bromodeoxyuridine (BrdU) and transferred to housing tanks with fresh facility water until the time of killing. Following a 2-h (Figs 6D and 7D; proliferation) or 2-week (Figs 6H and 7M; differentiation) period post-BrdU injection, animals were killed and brain tissue processed for immunohistochemistry. Conversely, zebrafish allocated for experiments examining survival of newly differentiated neurons were injected with BrdU as above on day 1 then left in housing tanks under standard conditions until day 14 (Figs 6I and 7N). Thereafter, over days 15–21 animals were exposed to assays and then killed on day 22 for analysis. Following killing, all tissue was processed for immunohistochemistry.

Exposure of zebrafish to chemosensory or vision assays 2 weeks post-BrdU injection was based on earlier work in forebrain neurogenic niches, showing that the proportion of newborn neurons after 2 weeks began to decline across most niches (Lindsey *et al.*, 2012). Therefore, by exposing animals to chemosensory enrichment over this window we predicted that we may be able to either sustain or enhance the size of the *de novo* neuronal population, while in the case of monochromatic light we predicted that such a decline may be further exacerbated. During these experiments we made the assumption that 14 days post BrdU injection and prior to exposure to vehicle or chemosensory stimulants, the total size of the BrdU⁺/neuronal protein HuC/HuD (HuCD)⁺ population in the control and experimental group was equivalent.

Neurogenic niches studied

Four separate neurogenic niches residing in primary sensory structures within well circumscribed regions of the adult zebrafish brain were investigated (Figs 6B and C, and 7B and C; red portion of schematics). All neuroanatomical terminology and rostrocaudal boundaries are in accordance with Wullmann *et al.* (1996). Chemosensory processing niches resided within the OB (olfaction; ×23–50; primarily the glomerular layer, GL; Fig. 6B) and the LX (gustation; ×279–303; Fig. 6C), while visual processing niches were situated within the caudal periventricular grey zone (PGZ; movement,

shape, color; ×223; Fig. 7B) of the TeO and the torus longitudinalis (TL; light intensity; ×153–190; Fig. 7C). For qualitative analysis of glial labeling in the PGZ, cross-sectional levels rostral to level 223 were additionally assessed. Previous electrophysiological studies in goldfish, a close relative of the zebrafish, have shown convincing evidence that the PGZ and TL indeed process different types of visual input (Gibbs & Northmore, 1998) and, accordingly, we tested the effects of altered visual input on adult neurogenesis in these structures.

BrdU administration and brain processing

BrdU administration was performed by injecting a single 10-mm pulse of BrdU (Sigma) intraperitoneally at a volume of 50 µL/g body weight into fish anaesthetised with 0.04% tricaine diluted in facility water, to detect proliferating cells in the S-phase of the cell cycle. Immediately after injection, animals were monitored in a recovery tank until respiration and swimming returned to normal, then transferred back to their holding tank. Following chase periods, animals were killed and either placed directly into fresh 4% paraformaldehyde or transcardially perfused with ice-cold 1× phosphate-buffered saline (PBS; pH 7.4) and 4% paraformaldehyde, and brains excised. Thereafter, brains were prepared for cryosectioning and tissue sections were cut using a Leica Cryostat (Model CM3050; Richmond Hill, ON, Canada) at 20-µm intervals through the rostrocaudal axis for immunohistochemistry as described previously (Lindsey *et al.*, 2012).

Immunohistochemistry

To detect BrdU⁺ proliferating cells alone or that had differentiated into a neuronal phenotype within neurogenic niches, single-labeling or double-labeling of BrdU⁺ cells with the neuronal protein marker HuCD were carried out according to protocols described in Lindsey *et al.* (2012), with the modification that secondary antibodies were applied for 2 h at room temperature. The neuronal marker HuCD was used specifically for the purpose of identifying newborn neurons arising from the niche, and not to infer functionality of the population. For BrdU labeling alone, brain sections were incubated in rat anti-BrdU polyclonal primary antibody (1 : 1000; MCA2060; Serotec; Raleigh, NC, USA), followed by goat-anti-rat-Cy3 secondary antibody (1 : 400; Cederlane; Burlington, ON, Canada). For double-labeling with HuCD, the BrdU primary antibody was conjugated to goat anti-rat Cy2 (1 : 200; Cederlane), and tissue next labeled with monoclonal mouse-anti-HuCD (1 : 400, 16A11; Molecular Probes; Eugene, Oregon, USA), and incubated in goat anti-mouse Cy3 secondary antibody (1 : 400; Cederlane) the next day.

To examine the presence of glial populations within niches, the staining patterns of three different glial markers were studied in combination with BrdU labeling. S100β was applied as a general glial marker, while glial fibrillary acidic protein (GFAP) and glutamine synthetase (GS) were used as RG markers to investigate whether populations may exist in the niche. For S100β, tissue was rinsed in 1× PBS with 0.3% Triton-X and incubated in polyclonal rabbit anti-S100β (1 : 1000, Z0311; Dako; Dako North America Inc., CA, USA) overnight and goat anti-rabbit Alexa 555 secondary antibody (1 : 1000; Invitrogen; Burlington, ON, Canada) for 1 h at room temperature the next day. Labeling of GS was performed as per Lindsey *et al.* (2012) using a mouse anti-GS primary antibody (1 : 800, MAB302; Millipore; Billerica, MA, USA). For GFAP, the transgenic line *Tg[GFAP:green-fluorescent protein (GFP)]* was utilised and sections labeled with a chicken anti-GFP antibody diluted in rinse solution (1 : 1000; Invitrogen) overnight. Thereafter, BrdU

labelling was completed with the rat primary antibody conjugated to either a goat anti-rat Alexa 488 or Alexa 555 secondary antibody (1 : 1000; Invitrogen). For counterstaining, a 1 : 10 000 dilution of 4',6-diamidino-2-phenylindole diacetate (DAPI; 1 mg/mL) was applied to brain sections at room temperature for 10 min in the dark. All sections were mounted in 100% glycerol for visualisation and confocal imaging.

Transmission electron microscopy

Transmission electron microscopy was used to examine the ultrastructural profile of cells composing neurogenic niches located within the OB ($\times 50$), the caudal PGZ ($\times 219$ – 223) of the TeO, and LX of the hindbrain ($\times 290$ – 303). These niches were chosen as they represent the dominant sensory structures utilised by zebrafish to process sensory information from the external environment. The TL was not examined at the ultrastructural level in this study. Animals were perfused using ice-cold $1\times$ PBS followed by 3% glutaraldehyde primary fixative, and brains were excised. Following overnight fixing of tissue in 3% glutaraldehyde, specimens were rinsed in 0.1 M Sorenson's phosphate buffer and post-fixed for 2 h with 1% osmium tetroxide. Thereafter, tissue was rinsed and dehydrated through an ascending ethanol series, and then infiltrated with an ascending series of 100% ethanol and Spurr's epoxy resin. The next day, tissue was infiltrated with fresh Spurr's resin twice over a 6-h period and then flat-embedded and polymerised at 65 °C overnight.

Using a Leica EM UC6 ultramicrotome, 1- μ m semithin sections and 100-nm ultrathin sections were taken at the corresponding rostrocaudal level of each niche at 5- μ m intervals. At each interval, semithin sections collected onto glass slides were stained with 0.035% Toluidine Blue/Methylene Blue diluted in methanol, while ultrathin sections were collected onto copper grids for transmission electron microscopy. Ultrathin sections were stained with 3% uranyl acetate in 50% methanol for 45 min, followed by Reynold's lead citrate for 10 min, and then dried overnight. Imaging was done by using an HT7700 Hitachi Transmission Electron Microscope and images captured using EMIP v0522 Software. Brightfield images of semithin sections were taken on a Leica DMI 300B inverted microscope.

For analysis, the morphology of cells present in niches of OB, PGZ and LX were compared with the seven ultrastructural profiles (Type IIa, Type IIb, Type III, Type IVa, Type IVb, Type V and Type VI) previously described in forebrain neurogenic niches by Lindsey *et al.* (2012).

Cell counting and imaging

Imaging was performed using a Leica TCS SP5 or Nikon C1 confocal microscope. Quantification of BrdU⁺ cells was done by counting a minimum of every second section through the rostrocaudal neuroaxis of each niche at 40 \times magnification for each biological sample (Figs 6B and C, and 7B and C; entire red region of each niche). Due to the size of the PGZ, BrdU⁺ cells in individual hemispheres were counted then summed together to represent the total number for the entire brain section under investigation. To quantify the proportion of BrdU⁺/HuCD⁺ cells each niche was analysed from images taken at 100 \times magnification from two or more non-adjacent sections (Figs 6B and C, and 7B and C; black rectangles within red niches). To analyse double-labeling of BrdU⁺/HuCD⁺ cells, all BrdU⁺ cells and BrdU⁺/HuCD⁺ cells within a tissue section were counted within a single counting box positioned in a representative region of the niche, with the position of the counting box

maintained across like-niches of different biological samples. As BrdU labeling is specific to the nucleus while the neuronal marker HuCD is predominantly expressed cytoplasmically, co-labeling of BrdU⁺/HuCD⁺ cells were confirmed in orthogonal view. Thereafter, a ratio of the proportion of BrdU⁺/HuCD⁺ cells to the total BrdU⁺ population within the counting box was calculated for each biological sample, for each niche, and then used to obtain a group mean.

To evaluate the expression pattern of glial markers across niches, images were taken at 100 \times magnification in a minimum of four separate animals. From these images we evaluated both the presence and absence of each marker and their association with BrdU⁺ cells. These data were then compared with the ultrastructural profile of cells in the niche. Cell counting was completed by quantifying the number of cells present in 0.5- to 1- μ m z-stacks using the optical disector principle (West, 1999; Geuna, 2005) with LEICA APPLICATION SUITE ADVANCE FLUORESCENCE LITE 2.3.0 proprietary software. Images shown are maximum projections or orthogonal views where appropriate and were adjusted for brightness and contrast using ADOBE PHOTOSHOP 7.0 or IMAGEJ software.

Data transformation and statistical analysis

Values are expressed as mean \pm SEM. Pairs of means were compared using independent sample or paired-sample *t*-tests, with all tests performed on the raw data. Samples were considered significant at $P < 0.05$; statistical analyses were completed using SIGMAPLOT 11.0 and graphs made using Microsoft Excel 2003.

With the exception of graphs comparing chemosensory stimulants pre- and post-infusion in Fig. 5, all cell counting data was transformed to percentages of control for graphical representation and to facilitate interpretation of our results. For both BrdU⁺ cell counting data and the proportion of BrdU⁺/HuCD⁺ cells, means for each biological sample (control and experimental groups) were normalised to the group mean of all biological samples of the control treatment. These transformed values were then averaged across all control or experimental biological samples and finally converted to percentages for graphical representation. Therefore, on all graphs the control treatment is consistently set to 100%.

Results

Radial glia Type IIa cells are present in chemosensory niches of LX and OB but absent in the visual niche of PGZ

Transmission electron microscopy was used to examine the ultrastructural organisation and cell types composing sensory niches residing in the OB ($n = 3$), LX ($n = 2$) and PGZ ($n = 3$) of the TeO. Terminology and classification used for cell types is based on those described in Lindsey *et al.* (2012) (see Table S1). Features of each niche are described separately below.

OB

The niche of OB spanned the ventrolateral portion of the OBs between rostrocaudal levels 23 and 50 (Wullimann *et al.*, 1996), and was located primarily within the GL (Fig. 1A). Cell morphologies could be seen interspersed between sets of glomeruli or lying ventral to glomeruli next to the outer lining of the bulb (Fig. 1B), though no clear laminar organisation could be observed. Detailed examination of cell types revealed the presence of Type III cells with smooth, evenly distributed chromatin (Fig. 1C), a small number of Type IIa cells with characteristics of RG cells (Fig. 1D and

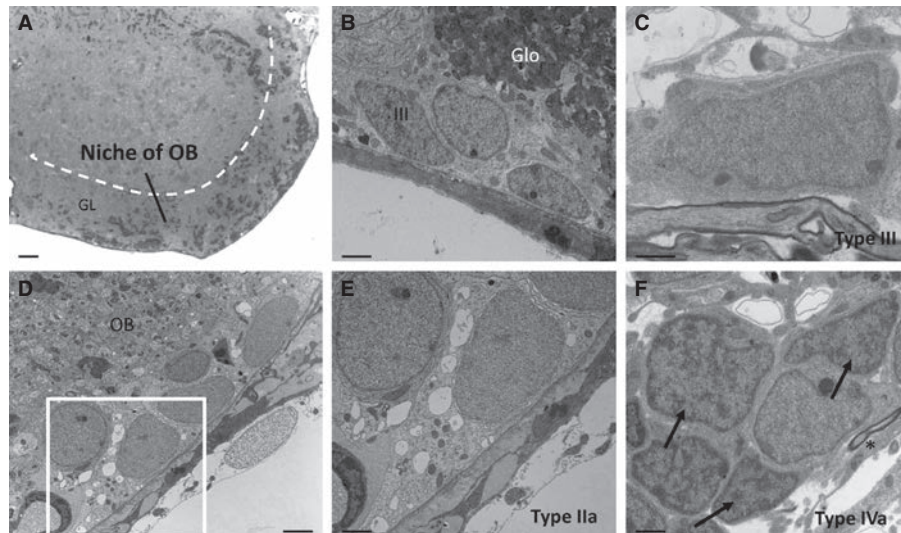


FIG. 1. Ultrastructural organisation and cell types of the adult neurogenic niche residing in the OB. (A) Brightfield semithin image of a single hemisphere of the OB. The niche is demarcated to the ventrolateral aspect of the bulb (white hashed line), made up primarily of the glomerular layer (GL) of the bulb. Dark clusters within the confines of the niche are glomeruli. (B) Cluster of cells in the ventral bulb, positioned below one or more darkly stained glomeruli (Glo). The morphological profile of a putative Type III cell can be seen. (C) Higher magnification image of a Type III cell. (D) Ventrolateral image displaying a collection of three putative Type IIa cells, one showing characteristic features including numerous large vacuoles and mitochondria in the cytoplasm (white box). (E) Higher magnification image from D (white box) showing ultrastructural details of a Type IIa cell in the OB. (F) Image depicting the chromatin organisation in Type IVa cells (black arrows). Evidence of a single cilium in longitudinal section is shown by the asterisk (*). In all images dorsal is up. Scale bars, 20 μ m (A); 2 μ m (B and D); 1 μ m (C, E and F).

E), as well as stereotypical clusters of Type IVa cells (Fig. 1F), and more rarely the presence of Type V cells (data not shown; see Fig. 2H). Evidence of a small number of cilia was also present in this niche; however, from the images analysed it was not possible to associate this structure with a given cellular profile.

LX

The niche of LX was positioned around the periphery of the LX, and spanned rostrocaudal levels 283–303 (Wullmann *et al.*, 1996). The lateral boundary of the niche was located adjacent the vagal nerve, with the niche continuing dorsally before extending ventromedially along the rhombencephalic ventricle (Fig. 2A). An epithelial lining consisting partially of squamous cells covered the niche dorsolaterally but terminated at the ventricle. Here, the niche consisted of three or four layers of mainly neurons, with a small number of non-neuronal phenotypes interspersed (Fig. 2B). At the dorsomedial aspect of the niche where the ventricular lumen began, the number of cell layers and cell morphologies increased (Fig. 2C), some of which included Type III cells (Fig. 2G) and Type V cells with darkly staining chromatin aggregated at the periphery of the nucleus (Fig. 2H).

Moving ventrally along the lateral wall few neurons were present, but a fairly continuous row of cells one or two layers deep, many having the ultrastructural profiles of Type IIa cells with visible microvilli, extended into the lumen (Fig. 2D and E). In a few instances, cells having characteristics of Type IIa but additionally displaying a single cilium extending from the cytoplasm were present (Fig. 2F). This indicates that either this is a novel cell type other than the Type IIa previously defined or cilia are not consistently detectable on this cell type.

PGZ

The niche of PGZ was located between rostrocaudal levels 219 and 223 (Wullmann *et al.*, 1996) deep to the superficial TeO, adjacent

to the tectal ventricle and opposite the eminentia granularis of the cerebellum (Fig. 3A). It was composed almost exclusively of a high density of both Type IVa and Type III cells that together spanned more than six cell layers deep (Fig. 3B, F and G). Extending along much of the border of the niche, a physical division between the irregular and elongated nuclei of Type III cells, many of which were oriented perpendicular to the tectal ventricle, and more deep Type IVa cells were conspicuous (Fig. 3C). Examination of the Type III cell population towards the margin of the niche showed that these cells were oriented parallel with the ventricle with distinctly elongated nuclear contours (Fig. 3D), displaying potential features of NE cells. For example, in a number of cases one pole of the nucleus of Type III cells was in contact with what appeared to be the apical membrane at the ventricular border, while the opposite end was positioned more basally, regardless of whether cells were oriented perpendicularly or parallel to the ventricle (Fig. 3C–E). Unlike Type III cells in neurogenic niches of the adult forebrain (Lindsey *et al.*, 2012), here these cells primarily made contacts with adjacent cells of this same morphology and deeper Type IVa cells. Infrequently, Type V cells were also noted within the niche (data not shown).

Glial markers are expressed exclusively in chemosensory niches but were absent from the visual niche of the caudal PGZ of the TeO

Glial markers displayed distinct patterns of expression in chemosensory niches (OB, LX) compared with the visual processing niche of the caudal PGZ. In both the niche of OB (Fig. 4A–E; $n = 4$ or 5 per marker) and LX (Fig. 4F–J; $n = 4$ –6 per marker), RG markers GFAP and GS, and S100 β , showed overlapping patterns of expression that were localised primarily to the domain of neurogenic niches where the density of cells was typically greatest (Fig. 4A and F), though a small number of labeled fibers or cell bodies extending into the external cellular layer of the bulb could be detected

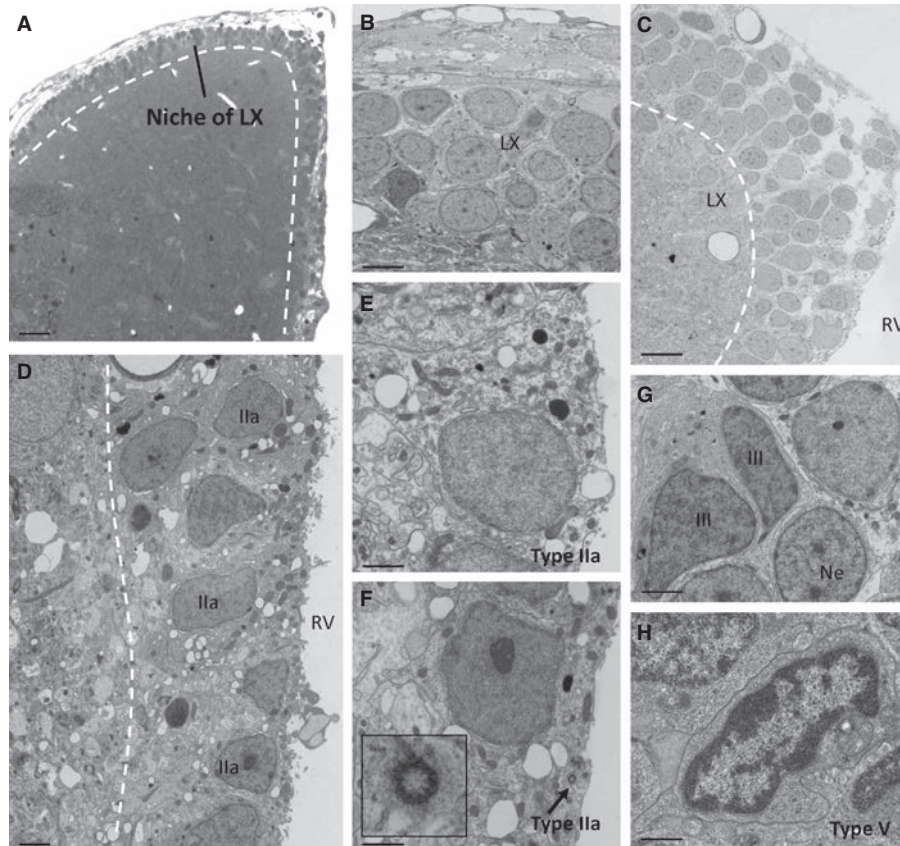


FIG. 2. Ultrastructural organisation and cell types of the adult neurogenic niche residing in the LX. (A) Brightfield image of a single hemisphere of the LX showing its stereotypical two- to five-cell-layered organisation and heterogeneity of cell types located dorsally in LX and continuing medially along the rhombencephalic ventricle. (B) Image depicting the dorsal epithelial lining devoid of ependymal cells with the niche of LX located ventrally and approximately three cell layers deep. (C) Dorsomedial corner showing an increase in the number of layers and cell types, and a narrowing as the niche continues medially along the rhombencephalic ventricle (RV). (D) Image showing a number of Type IIa cell morphologies in the periventricular zone of the niche of LX. (E) Higher magnification showing ultrastructural features of Type IIa cells. (F) Example of a putative Type IIa cell with a single cilium (black arrow) present in the cytoplasm. Inset shows higher magnification of cilium in cross-section. (G) Image showing two irregular shaped Type III cells with evenly distributed, light–medium colored chromatin adjacent to a neuron (Ne). (H) Image of an infrequently detected Type V cell with nuclear chromatin localised at the periphery. (G) In all panels, white hashed line depicts boundaries of the niche adjacent the parenchyma. White box in G shown in orthogonal view in G'. In all images dorsal is up. Scale bars, 16 μm (A); 4 μm (B and C); 2 μm (D); 1 μm (E–H).

(Fig. 4B–D). This same pattern of GFP⁺ expression in the adult OB has been shown previously in the zebrafish with GFAP reporter lines, and it has also been shown that the staining pattern is representative of endogenous GFAP labeling (Lam *et al.*, 2009). GFAP labeling using the transgenic line *Tg[GFAP:GFP]* most clearly revealed positively-labeled cell bodies and fibers in chemosensory niches (Fig. 4B and G). In the niche of LX specifically, one or two layers of GFP⁺ cells could be observed residing along the rhombencephalic ventricle, with processes emanating into the parenchyma (Fig. 4G, inset), suggestive of RG-like stem/progenitor cells. By double-labeling glia with the S-phase marker BrdU we additionally showed that glial labeling occurs in the same domain as BrdU⁺ labeling following 2-h pulse-chase experiments, and that subpopulations of BrdU⁺/glial-positive cells can be reliably observed among chemosensory niches (Fig. 4E and J), and that this was consistent for all three glial markers (data not shown).

Compared with the pattern of RG-like labeling across chemosensory niches, the caudal PGZ (level 223) was devoid of any detectable RG-like or S100 β expression at the border of the tectal ventricle where BrdU⁺ populations reside (Fig. 4K–O; $n = 4–7$ per marker). Notably, many of the BrdU⁺ cells displayed elongated nuclei which were often orientated parallel to the ventricle (Fig. 4O), with more ovoid BrdU⁺ nuclei observed one or two rows

deeper, in agreement with the ultrastructural morphology and position of Type III and Type IVa cells (see Fig. 3D). More rostrally (level 219) staining with antibodies against GS could be seen as the PGZ began to enlarge (Fig. 4R), though RG-like labeling and BrdU⁺ labeling remained separate (Fig. 4T). At cross-sectional level 213 and extending rostrally throughout the TeO, all glial markers displayed prominent labeling within the PGZ as this structure formed an arc and extended away from the tectal ventricle (Fig. 4Q and S; GS data not shown). GFP labeling further illustrated that both cell bodies and processes located deep to the PGZ at cross-sectional level 213 in the central and ventrolateral nucleus of the torus semicircularis were positive for GFAP (Fig. 4Q). The absence of RG-like labeling in the caudal neurogenic niche of PGZ, in particular markers GFP and GS, along with the elongated nuclear shape of many BrdU⁺ cells similar to Type III ultrastructural profiles, indicates that stem/progenitor cells of RG morphology do not reside within this niche at the rostrocaudal level examined in this study and that an alternative phenotype of ANSC is present.

Chemosensory stimulation enhances neuronal survival

To investigate whether chemosensory-specific stimuli had an effect on stages of adult neurogenesis, zebrafish were exposed to 7-days of

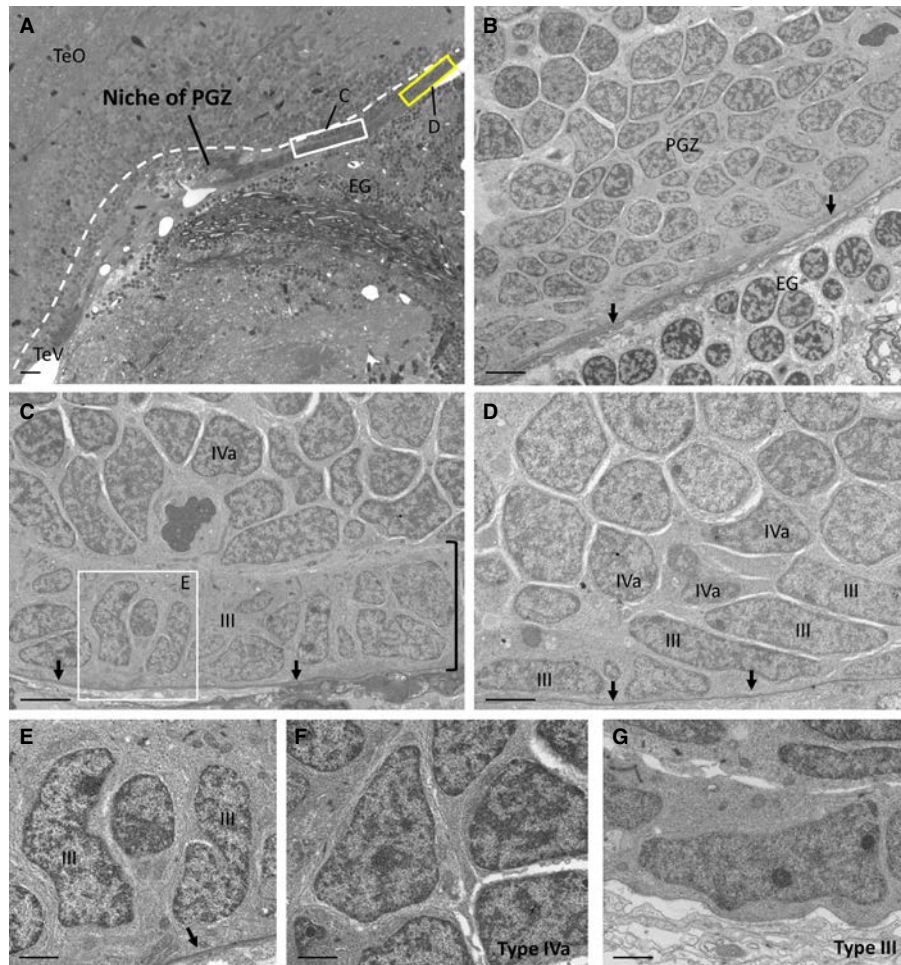


FIG. 3. Ultrastructural organisation and cell types of the adult neurogenic niche residing in the PGZ of the TeO. (A) Brightfield image showing the location of the niche of PGZ in the deep layers of the TeO (white hashed lines) adjacent the midbrain tectal ventricle (TeV) and opposite the eminentia granularis (EG) of the cerebellum. White and yellow rectangles shown at higher magnification in C and D, respectively. (B) Representative image of the niche composed of eight to ten cell layers deep, originating from the ventricular lining and consisting primarily of Type IVa and Type III cellular profiles. (C) Higher magnification image of white box in A depicting physical division between outer layer of the niche of PGZ composed of irregular shaped Type III cells (black bracket) and deeper layers of niche where clusters of Type IVa cells reside. (D) Higher magnification of yellow box in A showing stereotypical elongated Type III cells located at the margin of the niche where the number of cell layers decreases, and oriented parallel to the ventricle, adjacent deeper Type IVa cells. (E) Higher magnification of white box shown in C depicting two representative Type III cells aligned perpendicular to the ventricle with one pole of the nucleus located at the apical membrane. (F, G) Higher magnification of the cellular morphologies of (E) Type IVa and (F) Type III cells with their reticulated and evenly distributed chromatin, respectively. In all panels black arrows indicate the location of the apical membrane at the border of the tectal ventricle. In all images dorsal is up. Scale bars, 20 μm (A); 4 μm (B); 3 μm (C and D); 2 μm (E–G).

randomised chemosensory stimulation. Five chemostimulants that had a significant effect on the swimming activity of zebrafish were identified by screening a number of different compounds (Fig. 5A). These included acidic amino acids (Fig. 5B; $n = 7$; paired-samples t -test, $P = 0.01$), aromatic amino acids (Fig. 5C; $n = 10$; paired-samples t -test, $P = 0.05$), neutral amino acids (Fig. 5D; $n = 6$; paired-samples t -test, $P = 0.049$), TCA (Fig. 5E, $n = 8$; paired-samples t -test, $P = 0.012$) and bloodworms ($n = 7$; paired-samples t -test, $P = 0.0002$; data not shown). The behavioural response of zebrafish to stimulants exemplified by increased swimming activity indicated to us that animals could sense these compounds in their aqueous environment. No significant difference was noted in animals exposed to sodium taurodeoxycholate hydrate (data not shown; $n = 10$; paired-samples t -test, $P = 0.084$) or vehicle control (Fig. 5F, $n = 12$; paired-samples t -test, $P = 0.396$). The five chemosensory stimulants detected by zebrafish were then applied to form a randomised chemosensory assay (Fig. 6A).

Using the chemosensory assay, we next asked what might be the effect of chemosensory exposure on niches residing in the OB and LX (Fig. 6B and C) compared with PGZ at different stages of adult neurogenesis. The stem/progenitor population 2 h post-BrdU injection following 7-day chemosensory exposure showed no significant effect across any of the three niches (Fig. 6D–G; $n = 7$ –11; independent samples t -test: OB, $P = 0.213$; LX, $P = 0.776$; PGZ, $P = 0.497$). Additionally, no significant difference was observed in the proportion of BrdU⁺/HuCD⁺ cells 2 weeks after exposure (Fig. 6H; $n = 5$ –9; independent samples t -test: OB, $P = 0.932$; LX, $P = 0.542$; PGZ, $P = 0.907$). However, when we injected BrdU on day 1 and exposed animals to our 7-day chemosensory assay from days 15 to 21 to assess neuronal survival, we detected a significant increase in the number of new neurons that survived after 3 weeks exclusively in chemosensory niches of OB and LX (Fig. 6I–K; $n = 4$ –7; independent samples t -test: OB, $P = 0.028$; LX, $P = 0.018$; PGZ, $P = 0.440$). These data imply that chemosensory

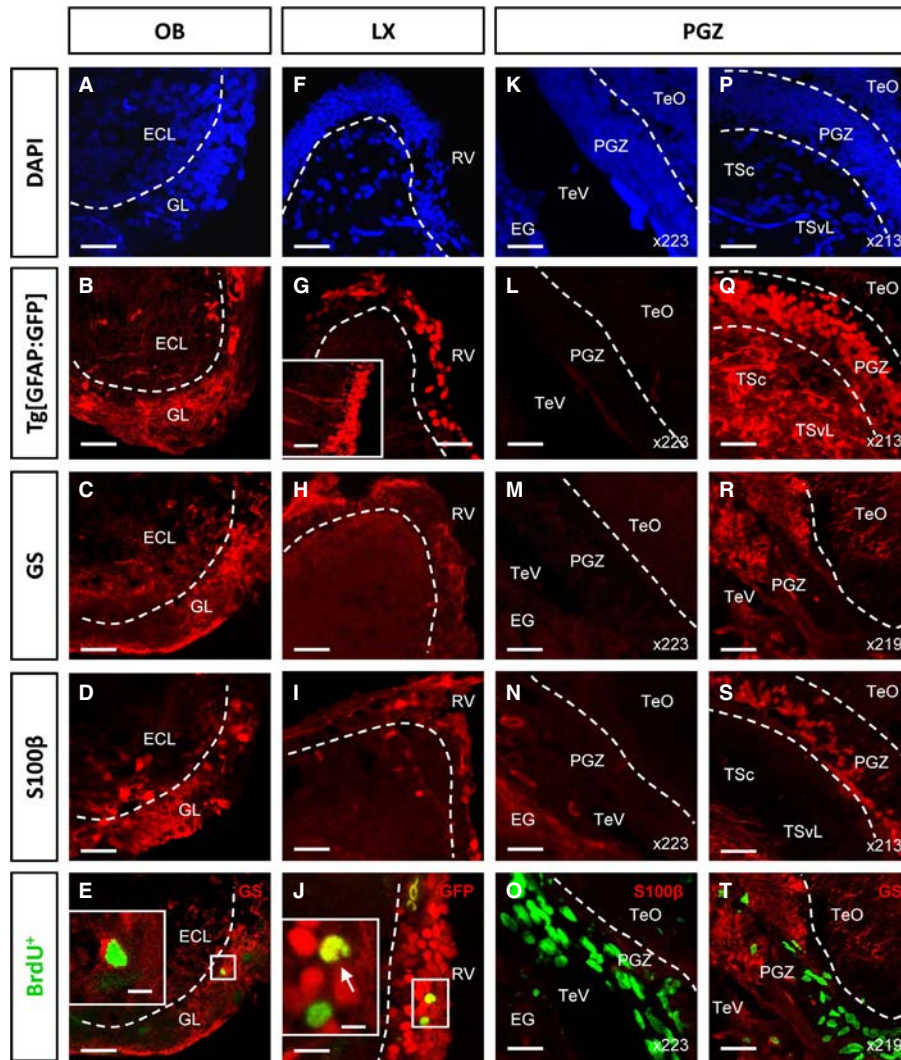


FIG. 4. Staining pattern of glial markers GFAP, GS and S100 β in neurogenic niches residing in chemosensory (OB, LX) and visual (PGZ) structures. (A, F, K and P) DAPI labeling showing cell density in sensory neurogenic zones located in OB, LX, PGZ (level $\times 223$) or more rostrally in the PGZ (level $\times 219$ – 213). (A–E) Niche of OB. (B–D) Glial markers were expressed predominantly within the region of the GL, with some diffuse labeling also present in the external cellular layer (ECL). (E) Representative example of a double-positive BrdU/GS cell following a 2-h pulse-chase period (inset). (F–J) Niche of LX. (G–I) Glial markers were localised dorsally and along the rhombencephalic ventricle (RV). (G) Labeling with the transgenic line *Tg[GFAP:GFP]* clearly demonstrated the presence of an RG subpopulation of GFP $^{+}$ cells two or three cell bodies deep at the ventricle, many with long radial processes extending into the parenchyma (inset). (J) Representative example of a double-positive BrdU/GFP cell near the ventricular surface (inset). (K–O) Caudal niche of PGZ ($\times 223$). (L–N) Absence of glial expression. (O) Stereotypical population of BrdU $^{+}$ /glial $^{-}$ cells positioned along the tectal ventricle (TeV) opposite the eminentia granularis (EG) of the cerebellum. A number of BrdU $^{+}$ cells were observed oriented parallel the TeV and with elongated nuclear contours. (P–T) Caudal PGZ at cross-sectional levels 219–213. (R, T) At level 219 BrdU $^{+}$ cells were still present at the margin of the niche but displayed no overlap with GS expression. (Q, S) More rostrally at level 213 as the PGZ extended inwards from the TeV, glial labeling of cell bodies was observed with all three markers (GS data not shown). (Q) GFP labeling showed that in addition to strong expression in the PGZ, a number of fibers and cell bodies were also labeled in the central (TSc) and ventrolateral nucleus of torus semicircularis (TSvL) of the TeO. In all images dorsal is up and white hashed lines demarcate the border of the niche. Scale bars, 10 μ m (A–E, G–J, K–O); 5 μ m (insets in E and J); 8 μ m (F, P–T, G inset).

exposure can function to enhance neuronal survival and that it acts in a modality-specific manner, specifically modulating niches residing in the corresponding primary sensory structure.

Monochromatic light and brightness induce changes in cell proliferation in the niche of PGZ and TL that correlate with the function of sensory structures

To examine whether changes from ambient lighting conditions (i.e. full spectrum light) perturbed physiological levels of adult neurogenesis in niches located within the PGZ and TL compared to the LX of zebrafish, we first exposed animals to 7 days of monochromatic

green or blue light alongside full-spectrum light intensity-matched controls (Fig. 7A–C). Exposure to monochromatic green light was sufficient to significantly decrease the BrdU $^{+}$ stem/progenitor population within the niche of the PGZ (Fig. 7D–F; $n = 6$ – 8 ; independent samples *t*-test, $P = 0.045$). However, no significant difference within TL (Fig. 7G; $n = 5$ – 9 ; independent samples *t*-test, $P = 0.529$) or LX (Fig. 6H; $n = 6$ – 10 ; independent samples *t*-test, $P = 0.561$) was observed. Conversely, exposure to monochromatic blue light produced no significant change in the stem/progenitor population across any of the three niches examined (Fig. 7D, G and H; independent samples *t*-test: PGZ, $n = 6$; $P = 0.561$; LX, $n = 4$ – 5 ; $P = 0.46$; TL, $n = 7$ – 8 ; $P = 0.524$).

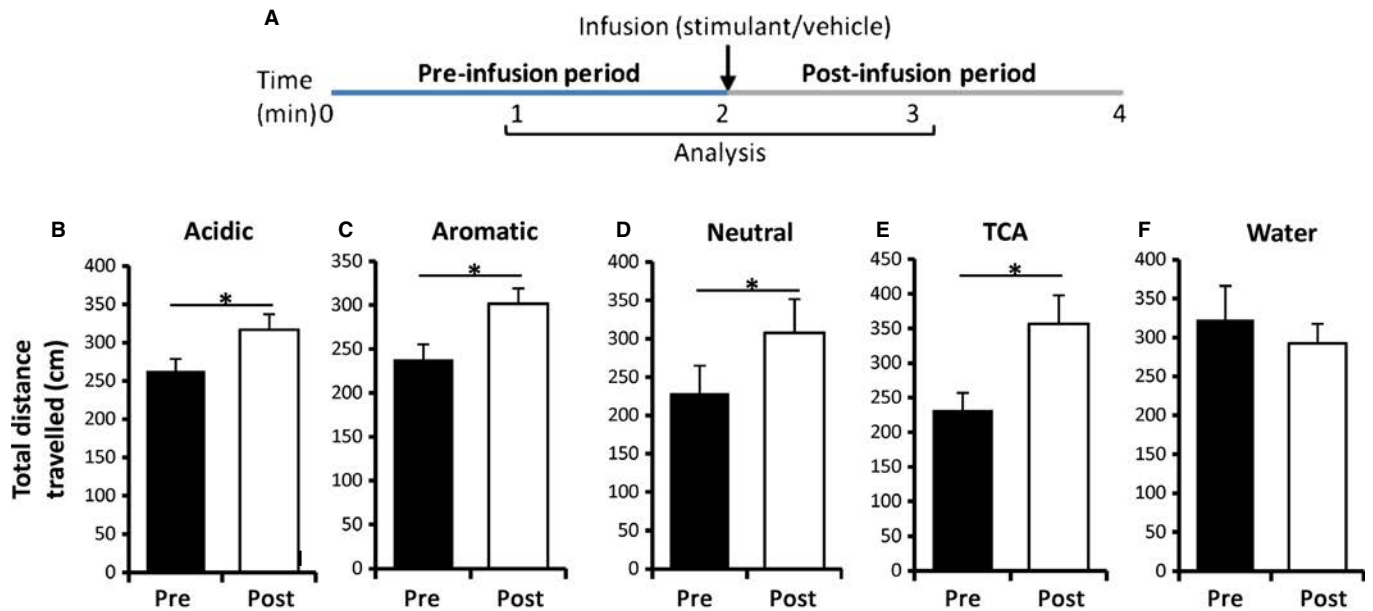


FIG. 5. Chemostimulants tested to which adult zebrafish responded. (A) Chemosensory assay designed to screen stimulants. Animals were exposed to a 2-min pre-infusion period of tank water and post-infusion period of the stimulant or vehicle control (water). Analysis of stimulus-evoked swimming activity was performed between minutes 1 and 2 of pre and 2–3 of post. (B–F) Chemosensory stimulants displaying a significant change in the total distance travelled by zebrafish compared to vehicle alone (F, water). * $P < 0.05$ (paired-samples t -tests).

For all treatments, niches of LX and TL displayed no change in the size of the BrdU⁺ population between full spectrum and monochromatic light for green (560 nm) or blue (480 nm) wavelengths, therefore we pooled these data and asked whether differences in light intensity (i.e. brightness – 200 vs. 15 lux) might affect the stem/progenitor pool of TL given its proposed role in detecting differences in light intensity (Gibbs & Northmore, 1998). Indeed, we noted that in the niche of TL (Fig. 7I and K; $n = 14$ or 15; independent samples t -test, $P = 0.001$), but not LX (Fig. 7L; $n = 9$ –16; independent samples t -test, $P = 0.282$), a significant decrease in the size of the BrdU⁺ proliferative population was observed. These findings support the notion that stem/progenitor proliferation in these niches changes according to the function of the sensory processing structure – PGZ decreasing with reduced color stimuli, TL decreasing with reduced irradiance.

As only monochromatic light in the peak wavelength for green light produced a significant difference in the size of the proliferative population in PGZ, we probed whether neuronal differentiation and survival may additionally be modulated in the absence of full spectrum light in this niche compared to the chemosensory processing niche of LX. In contrast to findings in niches of chemosensory structures, 7-day exposure to green light affected neither the proportion of newly differentiated neurons (Fig. 7M; $n = 3$ –5; independent samples t -test: PGZ, $P = 0.493$; LX, $P = 0.524$) nor the total number of newly derived neurons that survived 3 weeks post-BrdU injection (Fig. 7N; $n = 3$ –5; independent samples t -test: PGZ, $P = 0.573$; LX, $P = 0.285$). These results indicate that visual assays used here appear to modulate only adult neurogenesis at the level of stem/progenitor cell proliferation, but not later stages of this process.

Discussion

In the present study we demonstrate how adult neurogenic niches residing within primary sensory structures of the central nervous

system are composed and modulated by modality-specific stimuli. We illustrate that the cytoarchitecture of sensory niches residing in the OB, LX and PGZ of the tectum varies, but still appear to include many of the same cellular morphologies that compose fore-brain niches of the adult zebrafish. We reveal that the niche of LX most closely resembles the laminar organisation of pallial niches, with both LX and OB including Type IIa cellular profiles of putative RG stem/progenitors. By contrast, the composition of the caudal niche of PGZ aligns with the ultrastructural organisation of forebrain subpallial niches, made up largely of Type III cells positioned at the ventricle, reminiscent of neuroepithelia. By correlating the position of Type III cells with BrdU⁺ labeling and the absence of GFAP, GS and S100 β expression, our data provide support for a non-RG stem/progenitor population in the niche of PGZ at the caudalmost aspect of the TeO.

In the second part of this study, we aimed to investigate the properties of neurogenic plasticity in sensory niches. We present evidence that neurogenic niches residing in chemosensory (OB, LX) and visual processing (PGZ, TL) structures of the brain respond to changes in the external sensory environment in a modality-specific manner that is associated with the processing modality of sensory structures themselves, and that this occurs at distinct stages in the neurogenic process. Specifically, chemosensory niches demonstrated sustained neuronal survival of newly differentiated neurons with exposure to chemosensory assays, while visual-related niches displayed neurogenic plasticity of the stem/progenitor population following changes in the available wavelength of light and brightness, respectively. Additional studies will be crucial to test neuronal functionality and integration of *de novo* populations within primary sensory structures and whether they play a direct role in optimising modality-specific sensory information processing from the environment.

The results of our study are summarised in a model in Fig. 8, taking into account baseline levels of cell death and that progeny of the stem/progenitor pool may undergo either gliogenesis or neuro-

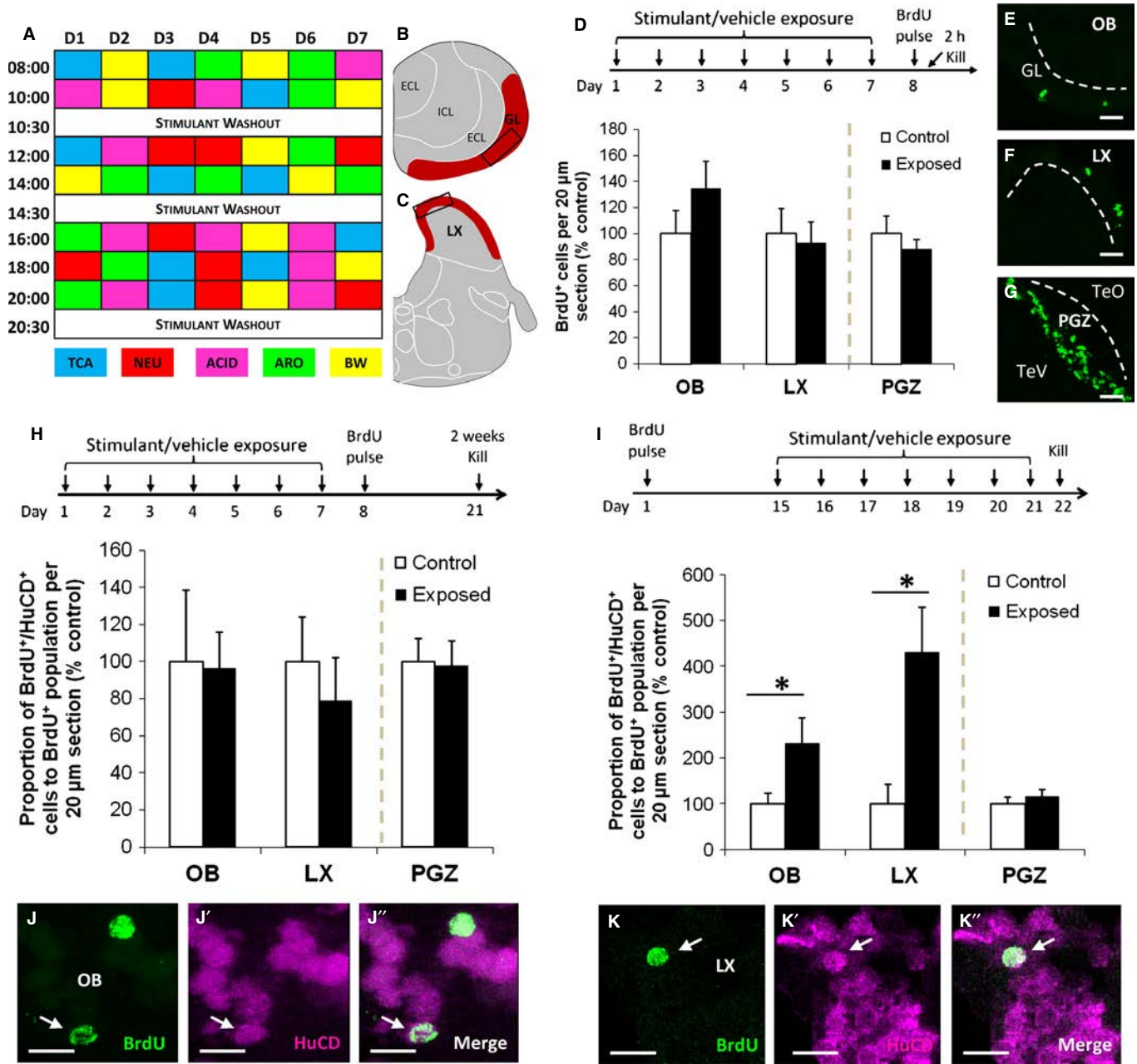


FIG. 6. Effects of chemosensory exposure on stages of adult neurogenesis in niches of OB, LX and PGZ. (A) Seven-day randomised chemosensory design. NEU, neutral; ACID, acidic; ARO, aromatic amino acids; BW, blood worms; TCA, sodium taurocholate hydrate. (B, C) Schematics showing the location of chemosensory niches in red within the primary sensory structures of (B) OB and (C) LX. For analysis, BrdU⁺ cells were counted throughout the niche (red), while co-labeling of BrdU⁺/HuCD⁺ cells was sub-sampled within niches (black rectangles). (D) Experimental protocol and results of chemosensory exposure on the stem/progenitor population. (E–G) Representative confocal images of BrdU⁺ cells within (E and F) chemosensory neurogenic niches and (G, negative control) the visual processing niche of PGZ. Dotted lines demarcate niche boundaries. (H) Experimental protocol and results of chemosensory exposure on neuronal differentiation. (I) Experimental protocol and results of chemosensory exposure on the survival of newborn neurons. (J–J'' and K–K'') Representative confocal images showing BrdU⁺/HuCD⁺ cells in chemosensory niches of OB (J–J'') and LX (K–K''). White arrows in panels show a co-labeled cell. ECL, external cellular layer; ICL, internal cellular layer; TeV, tectal ventricle. All graphical data are represented as percentages of control. In all images dorsal is up. **P* < 0.05 (independent samples *t*-tests). Scale bars, 10 μm.

genesis. Collectively, our findings raise the intriguing possibility that modulation of the neurogenic niche at specific stages of adult neurogenesis in sensory structures may be coupled with the phenotype of ANSCs present, such that niches characterised by RG profiles lead to changes in the survival of adult-born neurons whereas niches containing a NE-like stem/progenitor profiles are altered principally in the rate of cell proliferation.

Cellular plasticity of adult-born cells in sensory processing structures is governed by modality-specific stimulation

The OB of mammals has taught us many important lessons concerning how adult neurogenesis can play a functional role in processing a specific modality and its relevance for a number of natural behaviours (Gheusi *et al.*, 2009, 2013; Gheusi & Lledo, 2014; Sakamoto

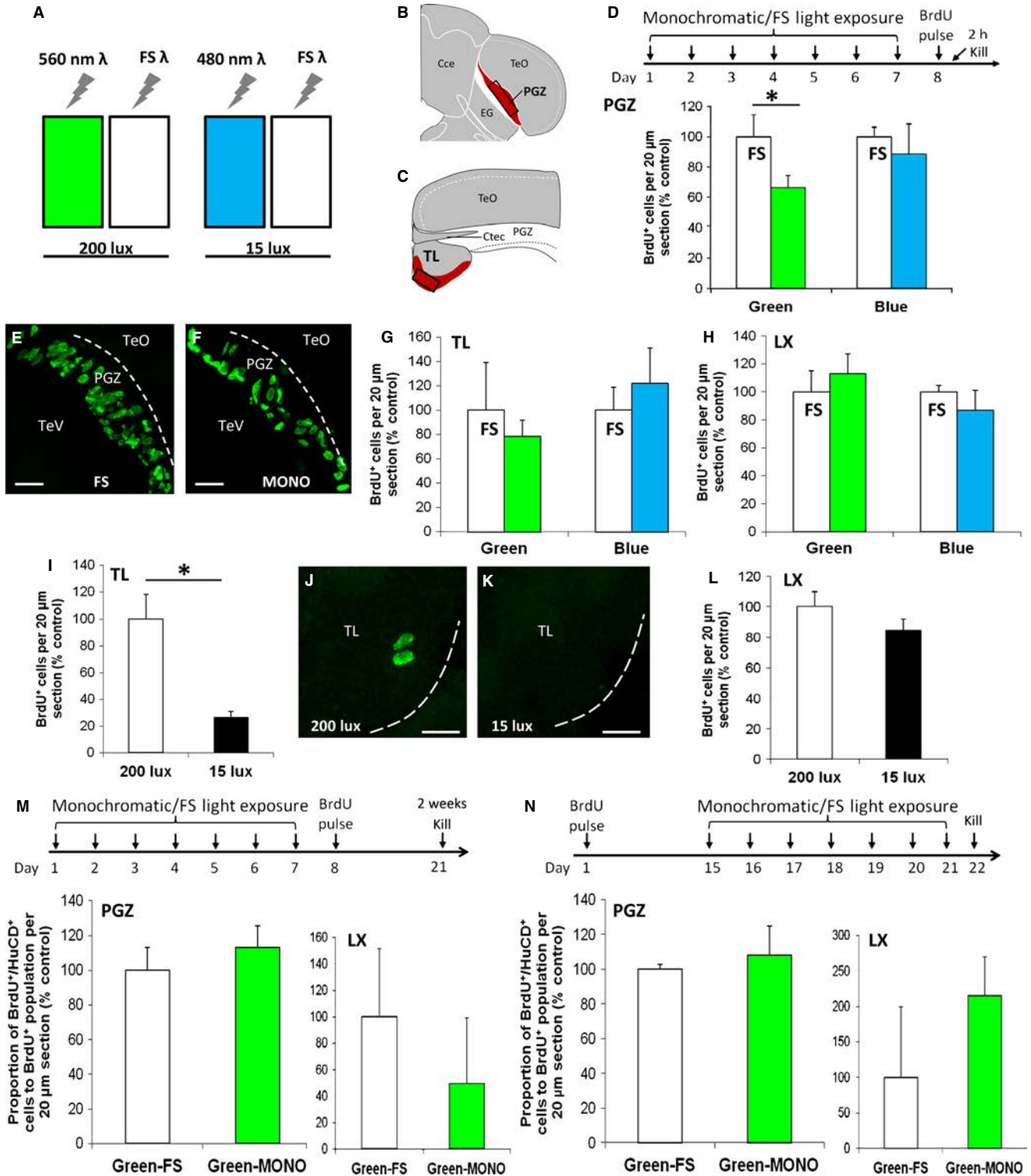


FIG. 7. Effects of monochromatic light and light intensity on stages of adult neurogenesis in PGZ, TL and LX. (A) Schematic of monochromatic light (green, 560 nm; blue, 480 nm) and intensity-matched full spectrum (FS) light stimuli to which zebrafish were exposed over 7 days. (B, C) Schematics showing the location of visual processing niches in red within the primary sensory structures of (B) PGZ and (C) TL. For analysis, BrdU+ cells were counted throughout the niche (red), while co-labeling of BrdU+/HuCD+ cells was sub-sampled within niches (black rectangles). (D) Experimental protocol and results of monochromatic light exposure on the stem/progenitor population in PGZ. (E, F) Representative confocal images of BrdU+ cells within the visual processing niche of PGZ between (E) FS and (F) monochromatic green light. Dotted lines demarcate boundaries of adjacent neuroanatomical regions. (G, H) Results of monochromatic light exposure on the number of BrdU+ cells in (G) TL and (H) LX (negative control). (I–L) Results of changes in light intensity (bright, 200 lux; dim, 15 lux) in niches of (I–K) TL and (L) LX (negative control). (J, K) Representative confocal images of a BrdU+ cell within TL under bright (200 lux, control) and dim (15 lux, experimental) conditions. Dotted lines demarcate the ventrolateral boundary of TL. (M) Experimental protocol and results of chemosensory exposure on neuronal differentiation. (N) Experimental protocol and results of chemosensory exposure on the survival of newborn neurons. TeV, tectal ventricle; Cce, corpus cerebella; EG, eminentia granularis; Ctec, commissura tecti. All graphical data are represented as percentages of control. In all images dorsal is up; **P* < 0.05 (independent samples *t*-tests). Scale bars, 10 μm.

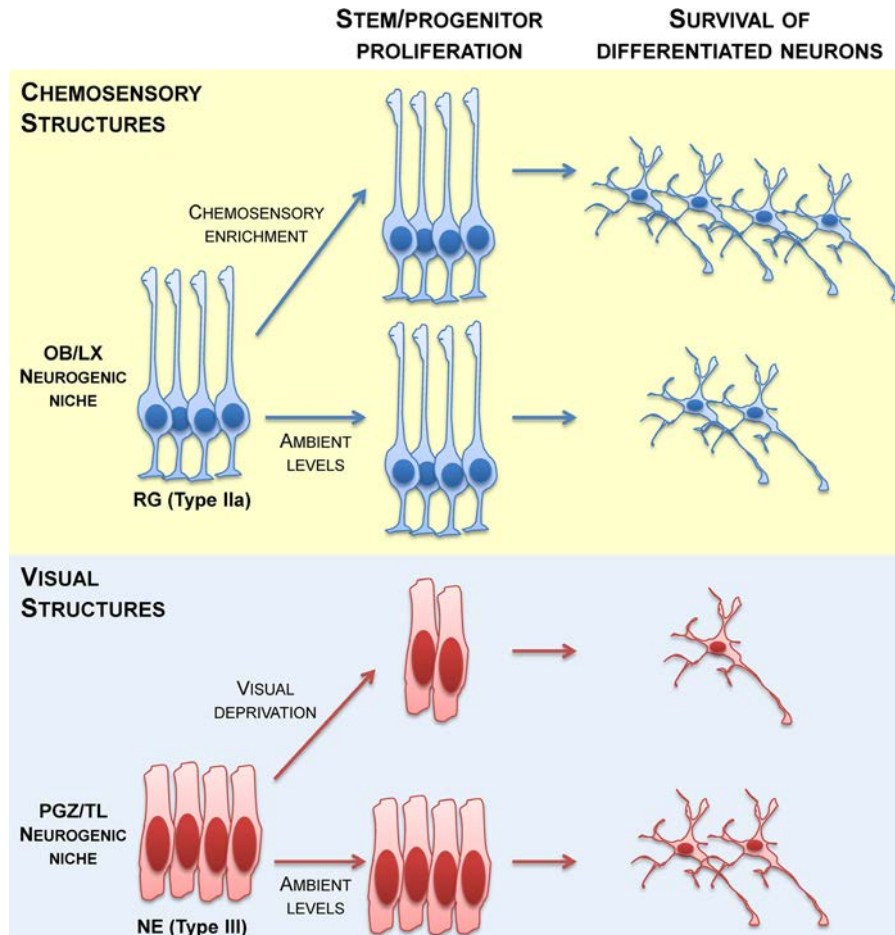


FIG. 8. Model summarising the major findings of our study between neurogenic niches residing in chemosensory and visual processing structures of the adult zebrafish brain. (Top) Neurogenic niches located within chemosensory processing structures of the OB and LX contain RG-like stem/progenitor cells of Type IIa ultrastructural morphology that upon chemosensory enrichment produce a greater number of surviving newly differentiated neurons compared with ambient levels of chemosensory input. (Bottom) Neurogenic niches located within visual processing structures of the PGZ of the TeO and TL contain NE-like stem/progenitor cells of Type III ultrastructural morphology that upon visual deprivation produce a decrease in the size of the stem/progenitor population compared with ambient levels of visual input. In the case of TL, direct ultrastructural evidence for the stem/progenitor phenotype is still pending, although we predict it to be similar to PGZ. Niches of both chemosensory and visual structures take into account the presence of baseline levels of cell death and the fact that not all stem/progenitor cells will generate a differentiated neuronal phenotype (shown here as a 2 : 1 ratio of progenitors to differentiated neurons under ambient, control, conditions).

et al., 2014b). It remains an open question, however, whether non-olfactory sensory processing brain regions harbouring progenitor/stem cells in adulthood also display properties of innate plasticity, and whether there is a functional role of *de novo* neurogenesis in behaviours that depend on these alternative sensory modalities. These questions can be suitably addressed using zebrafish and other teleost species, given their widespread adult neurogenesis.

A fundamental difference between neurogenesis in the bulb of mammals compared with structures such as the LX and TeO is that the major reserve of ANSCs in the bulb are born distally in the subependymal zone (SEZ) of the lateral ventricles (Lois & Alvarez-Buylla, 1994), not locally within the bulb. This has important repercussions for the influence of the surrounding environment on populations of cells at different stages of adult neurogenesis in terms of both molecular signals and cell-to-cell communication that could drive the degree of plasticity or potential fate of differentiating cells. At present, we know very little about this outside of the mammalian OBs. By better understanding the cellular plasticity of adult sensory niches in teleosts we have the opportunity to uncover mechanisms that may help to understand why adult neurogenesis is so restricted in mammals.

Accumulating evidence in vertebrates demonstrate that in many instances neurons derived from adult stem cell niches appear to be involved in fulfilling a species-specific biological role. For instance, hippocampal neurogenesis is associated with learning and memory function in mammals by the addition of new neurons (van Praag *et al.*, 1999; Garthe *et al.*, 2009; Stone *et al.*, 2010; Martinez-Canabal *et al.*, 2012; Vadodaria & Jessberger, 2014), with paternal–adult offspring recognition shown to necessitate increases in both olfactory and hippocampal neurogenesis (Mak & Weiss, 2010). In songbirds, new song learning requires seasonal replacement of newborn neurons (Paton & Nottebohm, 1984; Nottebohm & Alvarez-Buylla, 1993; Nottebohm & Liu, 2010). In contrast, food storing (Hoshooley *et al.*, 2007; Sherry & Hoshooley, 2009; Barnea & Pravosudov, 2011) and migratory (LaDage *et al.*, 2011) birds show increases in the number of newborn neurons recruited into the hippocampus to facilitate memory retrieval of food caches or migratory route, respectively. In some instances, however, a relationship between adult neurogenesis and a predicted biological role have been absent (Amrein & Lipp, 2009). For example, a surprisingly large number of bat species lack neurogenesis in the hippocampus

(Amrein *et al.*, 2007), even though under both wild and laboratory conditions they display precise spatial memory for food sources (Thiele & Winter, 2005). Moreover, cetaceans, such as whales, which are known to make extensive long-distance migrations through the ocean, also show no evidence for adult hippocampal neurogenesis to date (Patzke *et al.*, 2013).

The notion that the birth of new neurons in the adult teleost brain may be functionally related to the processing demand of the external environment continues to be overshadowed by the widespread belief that such species undergo lifelong neurogenesis in an additive manner solely for the purpose of growth. Though indeterminate growth is a common feature of many teleost species (Patnaik *et al.*, 1994; Zupanc, 1999, 2006; Kaslin *et al.*, 2008; Zupanc & Sirbulescu, 2011; Johnston *et al.*, 2014), this does not exclude the possibility that a subset of these neurons may additionally fulfill a more active role in brain processing rather than only passive growth. Earlier studies in cyprinids and cichlids have shown strong correlations between the sizes of brain structures, in particular those related to sensory processing, and the lifestyle, microhabitat and social structure of the species (Brandstatter & Kotschal, 1989, 1990; Kotschal & Palzenberger, 1992; Huber *et al.*, 1997; Kotschal *et al.*, 1998; Pollen *et al.*, 2007). These experiments suggest that more neurons might be added to those regions of the brain requiring specific processing demand; however, a relationship between brain size and adult neurogenesis, as well as the functional contribution of newborn neurons, has yet to be established.

In common with other models of adult neurogenesis, zebrafish have a wide repertoire of social behaviours that depend on chemosensory and visual processing. For instance, mating is triggered by photoperiod at dawn as well as pheromones released into the water, while shoaling preference and social status often involve a number of visual cues (Saverino & Gerlai, 2008; Spence *et al.*, 2008). During gustatory processing, zebrafish utilise an intraoral system with taste buds located on the oropharynx and gill arches, resulting in a more developed LX for taste processing in cyprinids (i.e. carp, goldfish) compared with silurids (i.e. catfish), which process this information in the facial lobe (Morita & Finger, 1985; Hayama & Caprio, 1989). The intimate relationship between sensory-dependent behaviours of zebrafish and the existence of adult neurogenic niches within processing structures of the OB, LX, TeO and TL provide a tractable system to investigate the behaviour of ANSCs and their progeny with changing sensory information.

A key finding of our study was that adult zebrafish exposed to chemosensory or visual assays displayed sensory-dependent neurogenic plasticity within niches situated in sensory processing structures. Particularly, we show that unimodal sensory stimuli affect only sensory niches that process the corresponding modality. For instance, an enriched chemosensory environment evokes neurogenic plasticity only in niches of OB and LX (but not PGZ), whereas deprivation of visual input in the form of the available spectrum of light or brightness of the environment altered only niches residing in visual processing structures of the brain, including the PGZ and TL (but not LX). Moreover, preliminary studies examining a number of forebrain structures in the zebrafish brain following exposure to chemosensory assays also showed that neurogenesis went unchanged (B.W. Lindsey & V. Tropepe, unpublished data). The niche-specific effect revealed here provides support for the hypothesis that constitutively active adult neurogenesis in sensory structures could be related to the sensory processing function of these brain centers and potentially contribute to a biologically relevant role for the animal.

It is conceivable that the functional stability of the adult brain would be disrupted if external and internal modulators induced a global affect across neural stem cell compartments and related circuitry, rather than only those niches responsible for processing a given modality, assuming new neurons arising from these niches played an integral role in information processing. Recent studies have shown that even *de novo* neurogenesis in a single niche, such as the rodent hippocampus, has the potential to impede retrieval of past memories by interfering with pre-existing circuitry (Frankland *et al.*, 2013). Thus, the importance of how environmental stimuli can evoke restrictive neurogenic plasticity in a single pertinent niche or in a more widespread manner across multiple niches of the adult brain cannot be ignored. Future experiments will be instrumental in elucidating whether cells derived from adult neurogenic niches in sensory structures functionally contribute to sensory processing or are simply bystanders in this process.

Stage-specific modulation of adult neurogenesis distinguishes chemosensory niches from visual processing niches

A surprising result of our study was that, in addition to niches being modulated by relevant modality-specific sensory input, chemosensory processing niches of OB and LX were differentially altered by the sensory environment compared with visual processing niches of PGZ and TL. In OB and LX, increases in chemosensory stimuli were positively correlated with increases in the surviving population of newborn neurons, whereas our data show that reduced visual input gives rise exclusively to decreases in the stem/progenitor pool in niches of PGZ and TL. One explanation that may account for this dichotomy could be the type of chemosensory or visual stimuli utilised. It is possible that different combinations of chemosensory enrichment or visual deprivation paradigms could induce changes at different stages in the neurogenic process, and that under certain conditions the same stage may be modulated in chemosensory and visual niches. An alternative hypothesis is that stage-specific differences in neurogenic plasticity are associated with the phenotype of stem/progenitor cells residing in the niche.

In agreement with our findings, previous studies in mice have shown that enhanced odor exposure has little influence on the size of the BrdU⁺ population following short-term 4-day chase experiments, but significantly increases the long-term survival of BrdU⁺ cells (Rocheffort *et al.*, 2002). Recent experiments have also revealed that the presence of newly derived populations of interneurons in the postnatal rodent OB appear to play an integral role in olfactory associative learning and memory (Sakamoto *et al.*, 2014a), suggesting the prospect of a similar role in chemosensory niches of the adult zebrafish brain. Studies in adult zebrafish have shown that the reverse experiment (i.e. removal of ambient olfactory stimuli) most directly effects the proportion of surviving neurons in the OB following ablation of afferent innervation from the olfactory organs, rather than changes in the proliferative pool (Villanueva & Byrd-Jacobs, 2009).

In the case of the OB, however, the source of ANSCs may not be limited solely to the bulb itself. A second population of stem/progenitor cells originating from the subpallial niche of the telencephalon appears to migrate into the bulb (Byrd & Brunjes, 1995, 1998, 2001; Adolf *et al.*, 2006; Grandel *et al.*, 2006; Kishimoto *et al.*, 2011). This parallels the trajectory of ANSCs from the SEZ to the OB in mammals along the rostral migratory stream (Lois & Alvarez-Buylla, 1994; Lois *et al.*, 1996), suggesting that the significant increase in neuronal survival displayed in the OB following chemosensory exposure cannot be definitively attributed to only the local

stem/progenitor population. Nevertheless, the consistent effect within LX whose niche is more tightly demarcated in the hindbrain indicates that chemosensory exposure does play a role in promoting survival of newly differentiated neurons.

We have previously shown that the size of the *de novo* neuronal population begins to decline in multiple forebrain niches 14 days post-BrdU injection (Lindsey *et al.*, 2012). This suggests that peak differentiation in newborn adult neurons has largely occurred by 14 days and that these neurons either persist or undergo cell death thereafter. In the present study we have asked whether we can alter the size of this differentiated population of newborn neurons by modality-specific sensory stimulation starting at 15 days post-BrdU injection. We speculate that any change in the proportion of BrdU⁺/HuCD⁺ cells as a result of the altered sensory environment in this paradigm is primarily due to changes in the survival of the differentiated newborn neurons. Thus, the increase we observed in the proportion of BrdU⁺/HuCD⁺ cells in chemosensory niches can be explained by increased survival of newborn neurons compared with controls that showed a population decline over days 15–21. However, there are two other possible explanations for our observations. First, chemosensory exposure may have promoted the differentiation of BrdU-retaining undifferentiated cells towards a neuronal fate in cases where these cells were not already committed by 14-days post-injection. Second, selective cell death of BrdU⁺/HuCD⁻ cells between days 15 and 21 of chemosensory exposure (but not in the controls) would result in a similar increase in the proportion of BrdU⁺/HuCD⁺ neurons. Although increased neuronal survival in the chemosensory niches of OB and LX is the most parsimonious explanation, without additional experiments we cannot completely rule out these alternative mechanisms.

The two visual processing niches examined here illustrate how the neurogenic responses of sensory niches segregate according to the type of visual information being encoded. By restricting the visual spectrum (i.e. full spectrum vs. monochromatic light) or altering the light intensity (i.e. bright light vs. dim), we demonstrate that the rate of stem/progenitor proliferation is modified in accordance with the level of stimuli reaching the PGZ and TL. Animals provided with monochromatic light in the green wavelength over a 7-day period produced a decrease in the stem/progenitor population in PGZ, but not TL. Conversely, experiments examining the contribution of light intensity on niches showed that TL displayed a significant reduction in the size of the proliferative pool under dim light conditions while the chemosensory niche of LX remained unchanged. Thus, these data show that the cellular plasticity and direction of change displayed by proliferative cells in the niche of PGZ compared with TL correlates with the level of stimuli received and processed by these sensory structures.

All layers of the PGZ are involved in encoding visual stimuli related to movement, shape and color (Wullimann *et al.*, 1996), but this information is primarily processed by the collection of neurons within the deep layer of the PGZ. In contrast, the TL, which is a midline outgrowth that develops from the TeO, has been implicated in processing changes in light intensity. Work in the goldfish, which shares a number of brain homologies with zebrafish (Rupp *et al.*, 1996), has shown at the electrophysiological level that the PGZ and TL do indeed respond to different forms of visual input (Gibbs & Northmore, 1998). Where the TL displayed spiking activity in response to changes in monochromatic stimulus radiance, spiking activity in the tectum showed increases at different rates across the spectrum, indicating sensitivity and functionality related to color dependence. In line with the function of these structures, a recent study examining sleep in zebrafish showed no significant difference

in cell proliferation in the TeO with exposure to either extended dark or light photoperiods compared to control animals (Sigurgeirsson *et al.*, 2013).

The zebrafish visual system is functional by 4–5 days post-fertilisation (Fleisch & Neuhauss, 2006). Already at this young age these animals contain four different cone types, as well as rods, that are morphologically distinct, and capable of responding to peak wavelengths for green, red, blue and UV (Nawrocki *et al.*, 1985; Fleisch & Neuhauss, 2006). In the present study, fish were exposed to either green or blue monochromatic light, but only an effect of monochromatic green light on stem/progenitor cell proliferation was observed. Studies have suggested that the strongest input to the tectum arises from green and red cones in zebrafish (Orger & Baier, 2005), and such differences may account for the current results. Our results agree with earlier studies in adult goldfish demonstrating that temporary unilateral optic nerve crush can lead to decreased levels of cell proliferation in the PGZ (Raymond *et al.*, 1983), and thus that ambient levels of visual input are required to sustain constitutive rates of stem/progenitor proliferation in the niche. Nonetheless, we cannot rule out the possibility that the proliferative population that is modulated with changes in visual stimuli is in fact a different subset of stem/progenitor cells than those detected under normal physiological conditions; however, this could not be distinguished in our experiments. Knowledge of how different wavelengths of light might influence photoreceptor cells in the retina that synapse with dendritic projections arising from the tectal niche that are associated with the stem/progenitor population in the PGZ remains to be resolved, but provides exciting avenues of study bridging retinal processing and functional adult neurogenesis in the tectum.

Can the phenotype of stem/progenitor cells predict stage-specific modulation of neurogenic niches in sensory structures?

One of the central aims of our study was to examine the ultrastructural organisation and cell types composing neurogenic niches present in the OB, LX and PGZ of the adult zebrafish brain. This analysis allowed us to postulate whether the cellular organisation of sensory niches might constitute the same cell types as those detailed previous in forebrain structures of the adult zebrafish (Lindsey *et al.*, 2012), as well as to evaluate a possible relationship between the identity of the stem/progenitor cell and stage-specific neurogenic plasticity within niches. We demonstrate that chemosensory neurogenic niches of OB and LX retained mainly the same cellular profiles as present in forebrain niches of the medial, lateral and dorsal zones of the dorsal telencephalon. Moreover, by correlating the position of specific cellular profiles at the ultrastructural level in these niches with immunohistochemical labeling of RG-like markers GFAP and GS, as well as S100 β , we show that a subpopulation of cells in chemosensory niches are indeed immunopositive for BrdU along with the respective glial markers, and that these cells appear to represent the phenotype of Type IIa RG-like stem/progenitor cells.

In the visual processing niche of PGZ, a strong parallel between the ultrastructural features of cell types in the subpallial niches of the anterior portion of the parvocellular preoptic nucleus and ventral nucleus of the ventral telencephalic area in the forebrain was observed (Lindsey *et al.*, 2012). This niche was made up primarily of multiple layers of Type III cells bordering the tectal ventricle and deeper layers of Type IVa cells, both of which markedly lacked any evidence of double-labeling of BrdU⁺ cells with glial markers, suggesting the absence of Type IIa cells similar to forebrain niches situated at the ventricular margin of the subpallium. This ultrastruc-

tural profile of proliferative Type III cells in the caudal PGZ of the tectum of zebrafish is consistent with previous work in the adult goldfish proliferative 'germinal' zone in this same structure (Raymond & Easter, 1983). At the caudalmost aspect of the PGZ where analyses were performed (i.e. level $\times 223$), we additionally observed a complete lack of glial labeling using GFAP, GS and S100 β . Where detection of BrdU⁺ cells subsided more rostrally in the PGZ, however, these markers readily stained populations of cell bodies and fibers.

Our results from the proliferative niche of the caudal PGZ using detailed cytoarchitecture investigations along with immunohistochemistry of glial markers indicates that the phenotype of stem/progenitor cells in this niche are of a non-RG nature. Although we are unable to definitively conclude that this BrdU⁺ proliferative population is composed of NE cells, several lines of evidence support the likelihood of this hypothesis. First, electron microscopy and immunohistochemistry showed that Type III cells were situated at the border of the tectal ventricle and often displayed an elongated nucleus. The same morphological profiles of adult neural stem/progenitor cells confirmed to be NE cells have been detected previously in the zebrafish cerebellum and tectum (Kaslin *et al.*, 2009; Ito *et al.*, 2010). Moreover, we have previously shown that cells with Type III ultrastructural profiles populate the neurogenic zone of the ventral telencephalon (Lindsey *et al.*, 2012), and that these cells undergo interkinetic nuclear migration (Ganz *et al.*, 2010). Second, in many cases one pole (i.e. apical) of the nucleus of Type III cells was in contact with apical membrane at the lumen, while the opposite end was positioned more basally. In addition to interkinetic nuclear migration, apical–basal polarity has been considered a seminal feature of NE cells (Gotz & Huttner, 2005). Work in the embryonic and adult zebrafish cerebellum (Kaslin *et al.*, 2009, 2013), and more recently in the lateral zone of the dorsal telencephalon (Dirian *et al.*, 2014), have shown immunopositive staining of stem/progenitor cells with a similar elongated nuclear profile using markers for zona occludens protein 1 (ZO-1), β -catenin and γ -tubulin (Kaslin *et al.*, 2009). Third, immunostaining showed that this population of BrdU⁺ cells did not double-label with any of the glial markers examined in our study, including GFAP, GS and S100 β . The lack of GFAP expression in particular has been considered a reliable indicator of an NE phenotype rather than transition to an RG cell, in proliferating cells localised to the ventricular zone during early development (Malatesta *et al.*, 2008).

Consistent with observations from a number of previous studies, we propose that a subpopulation of cells in the caudal PGZ having Type III cellular profiles and that are BrdU⁺ are strong candidates as NE stem/progenitor cells. This notion is further corroborated by previous studies in the adult zebrafish TeO that demonstrated PCNA⁺ proliferative populations with similar morphological characteristics located at the dorsal margin of the PGZ at cross-sectional levels slightly more rostral than investigated here (Ito *et al.*, 2010). Moreover, marker analysis showed that these cells were devoid of labeling with glial markers, including GFAP, but possessed canonically expressed apical–basal proteins such as ZO-1 and γ -tubulin. A similar finding has been reported in the medaka (Alunni *et al.*, 2010). Taken together, our data at the electron microscopy level in conjunction with immunohistochemistry demonstrate that adult neurogenic compartments of the central nervous system responsible for processing different forms of information (i.e. higher-order vs. sensory) appear to be made up of similar morphological profiles. This raises the question of whether the same cell type is governed by different molecular cues within the microenvironment of the niche in the forebrain compared with sensory domains.

In adult vertebrates, it has been confirmed that the phenotype of ANSCs in niches of the forebrain are astrocytes (SEZ of mammals), radial astrocytes (subgranular zone of mammals) or RG-like cells (reptiles, birds, fish; Doetsch *et al.*, 1999; Seri *et al.*, 2001; Garcia-Verdugo *et al.*, 2002; Kriegstein & Alvarez-Buylla, 2009; Ganz *et al.*, 2010; Marz *et al.*, 2010; Lindsey *et al.*, 2012; Grandel & Brand, 2013). The only exceptions to date appear to be in a small number of neurogenic compartments in teleosts that house NE-like stem/progenitor cells, including the cerebellum (Kaslin *et al.*, 2009, 2013), rostral PGZ (Alunni *et al.*, 2010; Ito *et al.*, 2010) and lateral zone of the dorsal telencephalon (Dirian *et al.*, 2014), as well as possible evidence for this NE-like morphology in subpallial niches of the zebrafish forebrain (Lindsey *et al.*, 2012). Thus, at present we may consider that adult stem cell niches in vertebrates consist of one of two classes of ANSCs, those with astrocytic/RG features or those having signatures of NE cells.

Our study suggests that the phenotype of the stem/progenitor cell (RG vs. NE) might be responsible for controlling which stage in the process of adult neurogenesis is modulated by the sensory environment. Here, we have shown that niches containing putative RG-like cells undergo plasticity at the level of neuronal survival (i.e. OB, LX), whereas niches housing possible NE-like profiles display changes in the proliferative population (i.e. PGZ). Earlier olfactory sensory deprivation studies in zebrafish (Villanueva & Byrd-Jacobs, 2009), along with assays used here exposing animals to a sensory-enriched environment, reveal a main effect at the level of neuronal survival in the bulb. Conversely, studies employing goldfish and zebrafish models have shown that removal of retinal fiber input or reductions in the available visual stimuli within the environment primarily lead to changes in the size of the stem/progenitor population in the PGZ of the TeO (Raymond *et al.*, 1983; Lindsey & Tropepe, 2014). Still, a richer understand of the properties of neurogenic plasticity in teleost models within neurogenic zones housing different ANSC populations is imperative before any conclusions can be drawn regarding a correlation between the neurogenic response and the local stem/progenitor phenotype. With our knowledge of adult neurogenesis in sensory structures of the vertebrate central nervous system beyond the bulb still in its infancy, many exciting avenues of enquiry await future study with the potential to contribute to stem cell biology and tissue regeneration.

Supporting Information

Additional supporting information can be found in the online version of this article:

Table S1. Morphological features of cell types characterised in forebrain neurogenic niches of the adult zebrafish brain as per Lindsey *et al.* (2012).

Acknowledgements

We thank Audrey Darabie in the Department of Cell & Systems Biology (University of Toronto, Canada) for her expertise with sample preparation and imaging for transmission electron microscopy experiments. A special thanks to Dr Aneil Agrawal of the Department of Ecology & Evolutionary Biology (University of Toronto, Canada) for the use of ETHOVISION 3.1 software, and Charmaine Fong for her assistance with analysis of zebrafish swimming behaviour for stimulant screening experiments. We would also like to thank Dr Nicolas Vespri, Mohsen Javam and Bonnie Chu for their participation during various facets of this project. Finally, thanks to the Australian Regenerative Medicine Institute (ARMI) at Monash University, Clayton campus for the use of the FishCore, and Monash Micro Imaging (MMI) facility for assistance with confocal imaging. Research funding was provided by the Natural Sciences and Engineering Research Council of Canada (NSERC).

Abbreviations

ANSC, adult neural stem cell; BrdU, bromodeoxyuridine; GFAP, glial fibrillary acidic protein; GFP, green-fluorescent protein; GL, glomerular layer; GS, glutamine synthetase; HuCD, neuronal protein HuC/HuD; LX, vagal lobe; NE, neuroepithelial; OB, olfactory bulb; PGZ, periventricular grey zone; RG, radial glial; SEZ, subependymal zone; TeO, optic tectum; TL, torus longitudinalis.

References

- Adolf, B., Chapouton, P., Lam, C.S., Topp, S., Tanhauser, B., Strahle, U., Gotz, M. & Bally-Cuif, L. (2006) Conserved and acquired features of adult neurogenesis in the zebrafish telencephalon. *Dev. Biol.*, **295**, 278–293.
- Alunni, A., Hermel, J.-M., Neuze, A., Bourrat, F., Jamen, F. & Joly, J.-S. (2010) Evidence for neural stem cells in the medaka optic tectum proliferation zone. *Dev. Neurobiol.*, **70**, 693–713.
- Amrein, I. & Lipp, H.P. (2009) Adult hippocampal neurogenesis of mammals: evolution and life history. *Biol. Letters*, **5**, 141–144.
- Amrein, I., Dechmann, D.K., Winter, Y. & Lipp, H.P. (2007) Absent or low rate of adult neurogenesis in the hippocampus of bats. *PLoS One*, **23**, e455.
- Barnea, A. & Pravosudov, V. (2011) Birds as a model to study adult neurogenesis: bridging evolutionary, comparative and neuroethological approaches. *Eur. J. Neurosci.*, **34**, 884–907.
- Blaser, R. & Gerlai, R. (2006) Behavioral phenotyping in zebrafish: comparison of three behavioral quantification methods. *Behav. Res. Methods*, **38**, 456–469.
- Brandstatter, R. & Kotschal, K. (1989) Life history of roach, *Rutilus rutilus* (Cyprinidae, Teleostei): a qualitative and quantitative study on the development of sensory brain areas. *Brain Behav. Evolut.*, **34**, 35–42.
- Brandstatter, R. & Kotschal, K. (1990) Brain growth patterns in four European cyprinid fish species (Cyprinidae, Teleostei: roach (*Rutilus rutilus*), bream (*Abramis brama*), common carp (*Cyprinus carpio*) and sabre carp (*Pelecus cultratus*). *Brain Behav. Evolut.*, **35**, 195–211.
- Byrd, C.A. & Brunjes, P.C. (1995) Organization of the olfactory system in the adult zebrafish: histological, immunohistochemical, and quantitative analysis. *J. Comp. Neurol.*, **358**, 247–259.
- Byrd, C.A. & Brunjes, P.C. (1998) Addition of new cells to the olfactory bulb of adult zebrafish. *Ann. NY Acad. Sci.*, **855**, 274–276.
- Byrd, C.A. & Brunjes, P.C. (2001) Neurogenesis in the olfactory bulb of adult zebrafish. *Neuroscience*, **105**, 793–801.
- Cachat, J., Stewart, A., Grossman, L., Gaikwad, S., Kadri, F., Chung, K.M., Wu, N., Wong, K., Roy, S., Suci, C., Goodspeed, J., Elegante, M., Bartels, B., Elkhayat, S., Tien, D., Tan, J., Denmark, A., Gilder, T., Kyzar, E., DiLeo, J., Frank, K., Chang, K., Utterback, E., Hart, P. & Kalueff, A.V. (2010) Measuring behavioral and endocrine responses to novelty stress in adult zebrafish. *Nat. Protoc.*, **5**, 1786–1799.
- Dirian, L., Galant, S., Coolen, M., Chen, W., Bedu, S., Houart, C., Bally-Cuif, L. & Foucher, I. (2014) Spatial regionalization and heterochrony in the formation of adult pallial neural stem cells. *Dev. Cell*, **30**, 123–136.
- Doetsch, F., Caille, I., Lim, D.A., Garcia-Verdugo, J.M. & Alvarez-Buylla, A. (1999) Subventricular zone astrocytes are neural stem cells in the adult mammalian brain. *Cell*, **97**, 703–716.
- Fleisch, V.C. & Neuhauss, S.C.F. (2006) Visual behavior in zebrafish. *Zebrafish*, **3**, 191–201.
- Frankland, P.W., Kohler, S. & Josselyn, S.A. (2013) Hippocampal neurogenesis and forgetting. *Trends Neurosci.*, **36**, 497–503.
- Ganz, J., Kaslin, J., Hochmann, S., Friedenreich, D. & Brand, M. (2010) Heterogeneity and Fgf dependence of adult neural progenitors in the zebrafish telencephalon. *Glia*, **58**, 1345–1363.
- Garcia-Verdugo, J.M., Ferron, S., Flames, N., Collado, L., Desfilis, E. & Font, E. (2002) The proliferative ventricular zone in adult vertebrates: a comparative study using reptiles, birds, and mammals. *Brain Res. Bull.*, **57**, 765–775.
- Garthe, A., Behr, J. & Kempermann, G. (2009) Adult-generated hippocampal neurons allow the flexible use of spatially precise learning strategies. *PLoS One*, **4**, e5464.
- Geuna, S. (2005) The revolution of counting “tops”: two decades of the disector principle in morphological research. *Microsc. Res. Techniq.*, **66**, 270–274.
- Gheusi, G. & Lledo, P.M. (2014) Adult neurogenesis in the olfactory system shapes odor memory and perception. *Prog. Brain Res.*, **208**, 157–175.
- Gheusi, G., Ortega-Perez, I., Murray, K. & Lledo, P.-M. (2009) A niche for adult neurogenesis in social behavior. *Behav. Brain Res.*, **200**, 315–322.
- Gheusi, G., Lepousez, G. & Lledo, P.-M. (2013) Adult-born neurons in the olfactory bulb: integration and functional consequences. *Curr. Top. Behav. Neurosci.*, **15**, 49–72.
- Gibbs, M.A. & Northmore, D.P.M. (1998) Spectral sensitivity of the goldfish Torus longitudinalis. *Visual Neurosci.*, **15**, 859–865.
- Gotz, M. & Huttner, W.B. (2005) The cell biology of neurogenesis. *Nat. Rev. Mol. Cell Biol.*, **6**, 777–788.
- Grandel, H. & Brand, M. (2013) Comparative aspects of adult neural stem cell activity in vertebrates. *Dev. Genes Evol.*, **223**, 131–147.
- Grandel, H., Kaslin, J., Ganz, J., Wenzel, I. & Brand, M. (2006) Neural stem cells and neurogenesis in the adult zebrafish brain: origin, proliferation dynamics, migration and cell fate. *Dev. Biol.*, **295**, 263–277.
- Hara, T.J. (1994) The diversity of chemical stimulation in fish olfaction and gestation. *Rev. Fish Biol. Fisher.*, **4**, 1–35.
- Hayama, T. & Caprio, J. (1989) Lobule structure and somatotopic organization of the medullary facial lobe in the channel catfish *Ictalurus punctatus*. *J. Comp. Neurol.*, **285**, 9–17.
- Hoshooley, J.S., Phillmore, L.S., Sherry, D.F. & MacDougall-Shackleton, S.A. (2007) Annual cycle of the black-capped chickadee: seasonality of food-storing and the hippocampus. *Brain Behav. Evolut.*, **69**, 161–168.
- Huber, R., van Staaden, M.J., Kaufman, L.S. & Liem, K.F. (1997) Microhabitat use, trophic patterns, and the evolution of brain structure in African cichlids. *Brain Behav. Evolut.*, **50**, 167–182.
- Ito, Y., Tanaka, H., Okamoto, H. & Ohshima, T. (2010) Characterization of neural stem cells and their progeny in the adult zebrafish optic tectum. *Dev. Biol.*, **342**, 26–38.
- Johnston, I.A., Bower, N.I. & Macqueen, D.J. (2014) Growth and the regulation of myotomal muscle mass in teleost fish. *J. Exp. Biol.*, **214**, 1617–1628.
- Kaslin, J., Ganz, J. & Brand, M. (2008) Proliferation, neurogenesis and regeneration in the non-mammalian vertebrate brain. *Philos. T. Roy. Soc. B.*, **363**, 101–122.
- Kaslin, J., Ganz, J., Geffarth, M., Grandel, H., Hans, S. & Brand, M. (2009) Stem cells in the adult zebrafish cerebellum: initiation and maintenance of a novel stem cell niche. *J. Neurosci.*, **29**, 6142–6153.
- Kaslin, J., Kroehne, V., Benato, F., Argenton, F. & Brand, M. (2013) Development and specification of cerebellar stem and progenitor cells in zebrafish: from embryo to adult. *Neural Dev.*, **8**, 1–15.
- Kishimoto, N., Alfaro-Cervello, C., Shimizu, K., Asakawa, K., Urasaki, A., Nonaka, S., Kawakami, K., Garcia-Verdugo, J.M. & Sawamoto, K. (2011) Migration of neuronal precursors from the telencephalic ventricular zone into the olfactory bulb in adult zebrafish. *J. Comp. Neurol.*, **519**, 3549–3565.
- Kotschal, K. & Palzenberger, M. (1992) Neuroecology of cyprinids: comparative, quantitative histology reveals diverse brain patterns. *Environ. Biol. Fish.*, **33**, 135–152.
- Kotschal, R., Van Staaden, M.J. & Huber, R. (1998) Fish brains: evolution and environmental relationships. *Rev. Fish Biol. Fisher.*, **8**, 373–408.
- Kriegstein, A. & Alvarez-Buylla, A. (2009) The glial nature of embryonic and adult neural stem cells. *Annu. Rev. Neurosci.*, **32**, 149–184.
- LaDage, L.D., Roth, T.C. & Pravosudov, V.V. (2011) Hippocampal neurogenesis is associated with migratory behavior in adult but not juvenile white-crowned sparrows (*Zonotrichia leucophrys* ssp.). *Philos. T. Roy. Soc. B.*, **278**, 138–143.
- Lam, C.S., Marz, M. & Strahle, U. (2009) *gfap* and *nestin* reporter lines reveal characteristics of neural progenitors in the adult zebrafish brain. *Dev. Dynam.*, **238**, 475–486.
- Lindsey, B.W. & Tropepe, V. (2006) A comparative framework for understanding the biological principals of adult neurogenesis. *Prog. Neurobiol.*, **80**, 281–307.
- Lindsey, B.W. & Tropepe, V. (2014) Changes in the social environment induce neurogenic plasticity predominantly in niches residing in sensory structures of the zebrafish brain independently of cortisol levels. *Dev. Neurobiol.*, doi: 10.1002/dneu.22183. [Epub ahead of print].
- Lindsey, B.W., Darabie, A. & Tropepe, V. (2012) The cellular composition of neurogenic periventricular zones in the adult zebrafish forebrain. *J. Comp. Neurol.*, **502**, 2275–2316.
- Lois, C. & Alvarez-Buylla, A. (1994) Long-distance neuronal migration in the adult mammalian brain. *Science*, **264**, 1145–1148.
- Lois, C., Garcia-Verdugo, J.-M. & Alvarez-Buylla, A. (1996) Chain migration of neuronal precursors. *Science*, **271**, 978–981.
- Mak, G.K. & Weiss, S. (2010) Paternal recognition of adult offspring mediated by newly generated CNS neurons. *Nat. Neurosci.*, **13**, 753–760.
- Malatesta, P., Appolloni, I. & Calzolari, F. (2008) Radial glia and neural stem cells. *Cell Tissue Res.*, **331**, 165–178.

- Martinez-Canabal, A., Akers, K.G., Josselyn, S.A. & Frankland, P.W. (2012) Age-dependent effects of hippocampal neurogenesis suppression on spatial learning. *Hippocampus*, **23**, 66–74.
- Maruska, K.P., Carpenter, R.E. & Fernald, R.D. (2012) Characterization of cell proliferation throughout the brain of the African cichlid fish *Astatotilapia burtoni* and its regulation by social status. *J. Comp. Neurol.*, **520**, 3471–3491.
- Marz, M., Chapouton, P., Diotel, N., Vaillant, C., Hesel, B., Takamiya, M., Lam, C.S., Kah, O., Bally-Cuif, L. & Strahle, U. (2010) Heterogeneity in progenitor cell subtypes in the ventricular zone of the zebrafish adult telencephalon. *Glia*, **58**, 870–888.
- Morita, Y. & Finger, T.E. (1985) Topographic and laminar organization of the vagal gustatory system in the goldfish, *Carassius auratus*. *J. Comp. Neurol.*, **238**, 187–201.
- Nawrocki, L., BreMiller, R., Streisinger, G. & Kaplan, M. (1985) Larval and adult visual pigments of the zebrafish, *Brachydanio rerio*. *Vision Res.*, **25**, 1569–1576.
- Nottebohm, F. & Alvarez-Buylla, A. (1993) Neurogenesis and neuronal replacement in adult birds. *Restor. Neurol.*, **6**, 227–236.
- Nottebohm, F. & Liu, W.-C. (2010) The origins of vocal learning: new sounds, new circuits, new cells. *Brain Lang.*, **115**, 3–17.
- Orger, M.B. & Baier, H. (2005) Channeling of red and green cone inputs to the zebrafish optomotor response. *Visual Neurosci.*, **22**, 275–281.
- Patnaik, N.K., Mahapatro, N. & Jena, B.S. (1994) Ageing in fishes. *Gerontology*, **40**, 113–132.
- Paton, J.A. & Nottebohm, F.N. (1984) Neurons generated in the adult brain are recruited into functional circuits. *Science*, **225**, 1046–1048.
- Patzke, N., Spocter, M.A., Karlsson, K.A., Bertelsen, M.F., Haagenen, M., Chawana, R., Streicher, S., Kaswera, C., Gilissen, E., Alagaili, A.N., Mohammed, O.B., Reep, R.L., Bennett, N.C., Siegel, J.M., Ihunwo, A.O. & Manger, P.R. (2013) In contrast to many other mammals, cetaceans have relatively small hippocampi that appear to lack adult neurogenesis. *Brain Struct. Funct.*, doi: 10.1007/s00429-013-0660-1. [Epub ahead of print].
- Pollen, A.A., Dobberfuhr, A.P., Scace, J., Igulu, M.M., Renn, S.C., Shumway, C.A. & Hofmann, H.A. (2007) Environmental complexity and social organization sculpt the brain in Lake Tanganyikan cichlid fish. *Brain Behav. Evolut.*, **70**, 21–39.
- van Praag, H., Christie, B.R., Sejnowski, T.J. & Gage, F.H. (1999) Running enhances neurogenesis, learning, and long-term potentiation in mice. *Proc. Natl. Acad. Sci. USA*, **96**, 13427–13431.
- Raymond, P.A. & Easter, S.S. Jr. (1983) Postembryonic growth of the optic tectum in goldfish. I. Location of germinal cells and number of neurons produced. *J. Neurosci.*, **3**, 1077–1091.
- Raymond, P.A., Easter, S.S. Jr., Burnham, J.A. & Powers, M.K. (1983) Postembryonic growth of the optic tectum in goldfish. II. Modulation of cell proliferation by retinal fiber input. *J. Neurosci.*, **3**, 1092–1099.
- Rochefort, C., Gheusi, G., Vincent, J.-D. & Leedo, P.-M. (2002) Enriched odor exposure increases the number of newborn neurons in the adult olfactory bulb and improves odor memory. *J. Neurosci.*, **22**, 2679–2689.
- Rupp, B., Wullmann, M.F. & Reichert, H. (1996) The zebrafish brain: a neuroanatomical comparison with the goldfish. *Anat. Embryol.*, **194**, 187–203.
- Sakamoto, M., Ieki, N., Miyoshi, G., Mochimaru, D., Miyachi, H., Imura, T., Yamaguchi, M., Fishell, G., Mori, K., Kageyama, R. & Imayoshi, I. (2014a) Continuous postnatal neurogenesis contributes to formation of the olfactory bulb neural circuits and flexible olfactory associative learning. *J. Neurosci.*, **34**, 5788–5799.
- Sakamoto, M., Kageyama, R. & Imayoshi, I. (2014b) The functional significance of newly born neurons integrated into olfactory bulb circuits. *Front. Neurosci.*, **8**, 1–9.
- Saverino, C. & Gerlai, R. (2008) The social zebrafish: behavioral responses to conspecific, heterospecific, and computer animated fish. *Behav. Brain Res.*, **191**, 77–87.
- Seri, B., Garcia-Verdugo, J.M., McEwen, B. & Alvarez-Buylla, A. (2001) Astrocytes give rise to new neurons in the adult mammalian hippocampus. *J. Neurosci.*, **21**, 7153–7160.
- Sherry, D.E. & Hoshoooley, J.S. (2009) The seasonal hippocampus of food-storing birds. *Behav. Process.*, **80**, 334–338.
- Sigurgeirsson, B., Porsteinsson, H., Sigmundsdottir, S., Lieder, R., Sveinsdottir, H.S., Sigurjonsson, O.E., Halldorsson, B. & Karlsson, K. (2013) Sleep-wake dynamics under extended light and extended dark conditions in adult zebrafish. *Behav. Brain Res.*, **256**, 377–390.
- Spence, R., Gerlach, G., Lawrence, C. & Smith, C. (2008) The behaviour and ecology of the zebrafish, *Danio rerio*. *Biol. Rev.*, **83**, 13–34.
- Stone, S.S., Teixeira, C.M., Zaslavsky, K., Wheeler, A.L., Martinez-Canabal, A., Wang, A.H., Sakaguchi, M., Lozano, A.M. & Frankland, P.W. (2010) Functional convergence of developmentally and adult-generated granule cells in dentate gyrus circuits supporting hippocampus-dependent memory. *Hippocampus*, **21**, 1348–1362.
- Thiele, J. & Winter, Y. (2005) Hierarchical strategy for relocating food targets in flower bats: spatial memory versus cue-directed search. *Anim. Behav.*, **69**, 315–327.
- Vadodaria, K.C. & Jessberger, S. (2014) Functional neurogenesis in the adult hippocampus: then and now. *Front. Neurosci.*, **8**, 1–3.
- Villanueva, R. & Byrd-Jacobs, C.A. (2009) Peripheral sensory deafferentation affects olfactory bulb neurogenesis in zebrafish. *Brain Res.*, **1269**, 31–39.
- West, M.J. (1999) Stereological methods for estimating the total number of neurons and synapses: issues of precision and bias. *Trends Neurosci.*, **22**, 51–61.
- Wullmann, M.F., Rupp, B. & Reichert, H. (1996) *Neuroanatomy of the Zebrafish Brain: A Topological Atlas*. Birkhauser Verlag Press, Basel, Switzerland, pp. 1–144.
- Zupanc, G.K.H. (1999) Neurogenesis, cell death and regeneration in the adult gymnotiform brain. *J. Exp. Biol.*, **202**, 1435–1446.
- Zupanc, G.K.H. (2006) Neurogenesis and neuronal regeneration in the adult fish brain. *J. Comp. Physiol. A.*, **192**, 649–670.
- Zupanc, G.K.H. & Sirbulescu, R.F. (2011) Adult neurogenesis and neuronal regeneration in the central nervous system of teleost fish. *Eur. J. Neurosci.*, **34**, 917–929.
- Zupanc, G.K.H., Hinsch, K. & Gage, F.H. (2005) Proliferation, migration, and neuronal differentiation, and long-term survival of new cells in the adult zebrafish brain. *J. Comp. Neurol.*, **488**, 290–319.